DOI: 10.1002/adfm.201806798
Article type: Review

Title: Printed solar cells and energy storage devices on paper substrates

Francesca Brunetti*, Alessandra Operamolla, Sergio Castro-Hermosa, Giulia Lucarelli, Valerio Manca, Gianluca Farinola, and Thomas M. Brown*

Prof. Francesca Brunetti, Sergio Castro-Hermosa, Giulia Lucarelli, Valerio Manca, Prof. Thomas M. Brown
CHOSE (Centre for Hybrid and Organic Solar Energy), Department of Electronic Engineering, University of Rome Tor Vergata, Via del Politecnico 1, 00133 Rome, Italy

E-mail: francesca.brunetti@uniroma2.it, thomas.brown@uniroma2.it
Dr. Alessandra Operamolla, Prof. Gianluca Farinola
Dipartimento di Chimica, Università degli Studi di Bari, via Orabona 4, I-70126 Bari, Italy

Keywords: flexible electronic, printed electronics paper, photovoltaics, energy storage, green electronics

Paper is a flexible material, commonly used for information storage, writing, packaging or specialized purposes. It also has strong appeal as a substrate in the field of flexible printed electronics. Many applications, including safety, merchandising, smart labels/packing, chemical/biomedical sensors, require an energy source to power operation. Here we review progress regarding development of photovoltaic and energy storage devices on cellulosic substrates where one or more of the main material layers are deposited via solution processing or printing. Paper can be used simply as the flexible substrate or, exploiting its porous fibre-like nature, as an active film by infiltration or co-preparation with electronic materials. Solar cells with efficiencies of up to ~ 4% on opaque and 9% on transparent substrates have been demonstrated. Recent developments in paper-based supercapacitors and batteries are also

reviewed with maximum achieved capacity of 1350 mF cm^{-2} and 2000 mAh g^{-1} respectively. Analysing the literature, it becomes apparent that more work needs to be carried out in continuing to improve peak performance, but especially stability and the application of printing techniques, even roll-to-roll, over large areas. Paper is not only environmentally friendly and recyclable, it is thin, flexible, low-weight, biocompatible, and low-cost.

1. Introduction

Paper is a flexible material, commonly used for information storage, writing, packaging or specialized purposes like, for instance, sanitary tissues. The main world manufacturers of paper are China (26.5% of the total), the European Community (22.5%), USA (17.9%) and Japan (6.5%) with an estimated world production of ≈420 billions of kg per year.[1] The starting pulp material, like the Northern Bleached Softwood Kraft (NBSK fibres), has a cost of ~1000-1100 $/t. Paper is produced by pouring a pulp slurry on a screen, followed by dewatering, pressing, and drying with the aid of a paper machine.[2] It is composed by a web of cellulose fibres, intimately interconnected thanks to the formation of inter-fibre hydrogen bonds. Paper is not only environmentally friendly and recyclable, it is thin, flexible, low-weight, ubiquitously available, biocompatible, biodegradable, has a low thermal expansion coefficient (CTE~28-40 ppm K^{-1})[3] and, most importantly, is low-cost: the final product has prices between (0.3–3 $/$m^2$).[4] Products made on paper are present from centuries in everyday life, but recently they have gained new interest due to the deep comprehension of their chemical and morphological properties.[2] This knowledge permits paper modification and its modern applications in innovative technologies. Paper represents an appealing substrate for flexible electronics: the thermal stability of cellulose, withstanding temperatures up to 250°C and decomposing at 300 °C, its recyclability can make it a preferable choice for some applications in comparison to more expensive plastics like poly(ethylene terephthalate) (PET).[5]

Furthermore, it exposes a high surface area for the absorption and storage of reagents. This opportunity makes paper very attractive for energy storage systems and all the related devices where high surface area is required. [6] Conversely, when considered for thin film devices application, standard uncoated paper presents some disadvantages, such as microscale surface roughness (1-10 micron), opaqueness, high porosity (10-30%) with large pores (1-5 micron), hygroscopicity, poor dimensional stability (1-5%) when moisture level in ambient changes [7]. The possibility to tailor paper characteristics allowed to mitigate some of these obstacles; for example, the surface roughness has been reduced applying coating layers, [8,9] or engineering papers based on microfibrils or nanofibrillated cellulose (NFC) which provide smoother substrates if compared to regular paper.[10]

The natural compatibility of paper with printing has allowed the application of several patterning techniques for the deposition on paper of active inks. Techniques as blade coating, slot die coating, spray coating, screen printing, inkjet printing, flexographic printing, gravure printing, dispenser printing, stencil printing have been demonstrated on paper offering also the possibility a straight path for scaling up of the production process.[11] The possibility of using paper as substrate for electronics has been proposed more than 50 years ago [12,13] however, it took more than 30 years to demonstrate the first simple electronic components and circuits, which was a smart pixel, on paper. [14] Nowadays, several devices have been demonstrated on paper such as thin film transistors, memories, organic light emitting diodes, sensors. [15,16,25,17–24]

The use of paper in electronics has followed two main approaches; in the first case, paper is used simply as the flexible substrate where the different devices are printed; in the second case additional functionalities are given to the cellulosic paper, such as for example transparency or conductivity, allowing its use as an active material.[10] For the realization of integrated systems, paper-based devices of different sizes often require the power supply; this aspect is crucial and has received increasing attention from the scientific community. [26] Several possible

technologies have been demonstrated as power supplies, in particular, photovoltaic devices, supercapacitors and paper batteries, represent a viable low cost route for printable energy generation and storage system on paper.[4,6,27–30]

The integration of solar cells into portable electronic devices and consumer products, such as sensors, gadgets, and smart objects, imposes a stringent requirement in terms of weight, mechanical properties and cost of photovoltaic (PV) devices. Ideally, solar cells should be fabricated by simple and cost-effective printing processes[31], and in a light-weight and flexible form, to enable a seamless integration into consumer electronics; moreover, the life cycle assessment of the device, and therefore its disposability, should be also taken into account when designing a solar device. In this context, paper act typically as substrate, becoming a solution for the low-cost, efficient and environmentally friendly electronics of the future, being abundant, renewable, recyclable, and simple and easy to fabricate and functionalize.

On the other side, storage devices, such as supercapacitors and Lithium based batteries, (Li-ion, Li-S and LiO_2), play a fundamental role due to ease of fabrication and integration with other electronic devices as well as providing excellent performances in terms of power and energy supplied.[6,32,33] These types of devices are typically formed of several parts: the electrodes (cathode and anode), the separator, the electrolyte, the current collector and the packaging.[34] Paper here, can act as a substrate for flexible electrodes, which can be printed with several techniques, as separator or, in the case of paper-like film structures, even as s self-standing paper based electrode. In the latter case, the electrodes are obtained assembling the conductive materials in a paper-like film structure. The porous surface of paper, can be exploited to infiltrate conductive materials as high effective area electrodes, facilitating electron collection, or as a separator facilitating ion transport. [6]

Other types of electrodes, often described as “paper-like” that include free-standing, self-supporting films made with electrically conductive materials (typically carbon based) do not

actually contain cellulose. The advantage of this type of electrode consists in a higher flexibility with respect to paper-based electrodes, higher electrochemical performances and lower resistivity, which make them promising for high power, high density energy storage devices. In this review, this type of electrodes will not be discussed, being out of scope; for an exhaustive analysis, please consider the paper of Yao et al. [34]

Here we will present a detailed analysis on the state of the art of the use of paper and cellulose-paper like systems for the realization of photovoltaic devices, supercapacitors and batteries where at least one of the main constituent layers has been deposited or synthesized via printing or solution processing techniques. In particular, we will cover research progresses on the engineering of paper as substrate for photovoltaic and storage devices (Section 2). Subsequently, the printing techniques that have been utilized so far for the manufacturing of these devices will be discussed in Section 3. Paper photovoltaics and storage will be presented in Section 4 and Section 5 respectively, while in Section 6 we will report on durability and recyclability issues.

2. Paper as substrate for printed light harvesting and energy storage devices

The substrate represents a key part in the fabrication of devices for energy harvesting and storage. Typically, the properties of the substrate have to be tailored considering different parameters such as the type of device, its durability, the architecture chosen, the deposition technique used and the technological process implemented. This leads to a wide variety of possible types of substrates that can be used. In the following subparagraphs, the attention is focused in particular on the use of paper-based substrates for the production of light harvesting and storage devices.

2.1 Light harvesting devices

Special surface treatments are necessary to enable opto-electronic thin film devices deposition on paper: first, it is necessary to decrease its natural surface roughness and porosity to ensure the efficiency of the printing process, reducing the risk of ink diffusion among paper pores by capillary action. Similarly, direct thermal evaporation of metal contacts would just result in penetration of the material into the paper's pores.[35] Active layer thickness and paper porosity control is important not only for cost reasons, but also to prevent cracks and defects in the conductive layers, that would drastically compromise the device performance. On the other hand, a highly smooth surface of the substrate may decrease the wettability of the printing solutions. Top coats of mesoporous inorganic structures, containing pigments and particles to improve the colour and/or light reflectivity of the surface are often applied on the surface of paper before ink deposition. Since water and oxygen infiltration in the devices can promote photo-oxidation of active materials or electrodes delamination, it is also necessary to confer cellulose paper low water vapour and oxygen transmission rates, i.e. encapsulant properties. The typical WVTR (water vapour transition rate) of cellulose is high (435-1209 g m^{-2} day^{-1} at 25 °C and 75% RH for 120μm NBSK paper),[36] and it can increase further in high humidity conditions. The coating layers are expected to improve on this issue.

The literature reports a variety of approaches to treat commercial paper or to prepare new cellulose products and composites producing an ideal electronic paper for use either as a substrate in thin film opto-electronic devices or energy storage devices. This literature is summarized in the **Table 1** and gives specific indication also on whether the biodegradability or recyclability of the device has been object of evaluation.

Table 1. Types of paper substrates suitable for optoelectronic or energy storage devices, their surface modification approach and specific applications.

Type of paper	Transparency	Commercial	Surface modification approach	Description of paper preparation/treatment	Average Surface Roughness[a]	Tensile strength[b]	Biodegradability/ Recyclability demonstration	Applications[a]	Refs
Specialty paper for electronics	NO	YES	Multilayer coating: resins; hydrophilic nanoporous coating; pigments	--	<20 nm	NA	Both	Perovskite SCs	[37]
		NO	Mineral pigment layer coated on top of a barrier latex layer	Reel-to-reel technique Calendering	55 nm	NA	Both	Hygroscopic insulator FET, printed OFET	[8,38,39]
Raw paper	NO	NO	Styrene acrylate and calcium carbonate/kaolin coating	Supercalendaring	9.42 nm	NA	None	Si thin film PV	[4]
	YES	NO	PDES (polymerizable deep eutectic solvent)	Screen printing	NA	>30 MPa	Only biodegradable	Printed circuits	[40]
	YES	NO	Ion gel infiltration	--	NA	NA	None	Electroluminescent devices	[41]
Newspaper	NO	YES	Parylene	Chemical vapour deposition/ Spin-coating	< 3 nm	NA	None	Photodiodes	[42]
Mulberry paper	NO	YES	Hydrophobic gold nanoparticles	Layer-by-layer assembly	NA	NA	None	Supercapacitors	[43]
Glossy paper	NO	YES	Zn/ZnO	Cold-foil transfer printing	80 nm	NA	None	All-Printed P3HT:PCBM OPV	[9]
Electrophoresis paper	NO	YES	Melted natural beeswax impregnation	--	NA	NA	Only biodegradable	Battery	[44]
Printing paper	NO	YES	--	Screen printing Ag NPs	NA	NA	Only biodegradable	Coplanar waveguides (CPWs)	[45]
			Zn/ZnO	Gluing	60 nm	NA	None	Solution processed OPV	[35]
			Amylum	Coated by manufatcturer	NA	NA	Only biodegradable	Solution processed OPV	[46]
			Pencil trace	--	NA	NA	Only biodegradable	Perovskite photodetector	[47]
			SWCNT or Ag nanorods	Wet treatment	NA	NA	None	Supercapacitors	[48]
	YES[d]	NO	Epoxy resin infiltration	Pressing	3 nm	> 60 MPa	None	Thin film inorganic PV	[20]
			Carboxymethyl cellulose infiltration	Pressing	0.9 nm	> 140 MPa	Only biodegradable	Substrate only	[49]
Tracing paper, Copy paper, tissue paper	NO	YES	PEDOT:PSS	Vapour oxidative deposition	NA	NA	None	OPV solar cell	[50]

Filter paper	YES[e]	NO	TEMPO-mediated oxidation	Swelling and pressing	NA	~ 100 MPa	Only biodegradable	OPV solar cell	[51]
			N,N-DMA and LiCl	Swelling and pressing	NA	>150 MPa	Only biodegradable	Substrate only	[52]
	NO	NO	Application of cellulose nanocrystals followed by fluorosilanes	Chemical vapour deposition	NA	NA	None	Substrate only	[53]
	NO	NO	Graphene nanosheet	Filtration method	NA	8.67 MPa	None	Supercapacitor	[54]
Nanopaper	YES[f]	NO	--	Pressing method	NA	223 MPa	Only biodegradable	Substrate only	[55]
					NA	NA	Only biodegradable	OPV solar cell	[56]
			TEMPO-oxidised	Pressing method	6.98 nm	NA	Only biodegradable	Perovskite solar cell	[57]
			TEMPO-oxidised and milled nanofibers	Filtration method	5 ÷7.7 nm	200 ÷ 400 MPa	Only biodegradable	OLED, OFETs	[19], [58]
			TEMPO-oxidised and milled nanofibers coated by bisphenol A-based epoxy resin	Filtration and Pressing	NA	NA	Only biodegradable	OTFTs	[22]
			-	Casting method-	7.9 ÷ 20.2 nm	NA	Only biodegradable	OPV solar cell	[59,60]
			-		1.8 ± 0.6 nm	NA	Both	OPVs	[61,62]
			--	Heating, pressing or casting method	NA	NA	Only biodegradable	OPV solar cell	[63]
			TEMPO-oxidised	From agro-industrial wastes	3.08 nm	NA	Only biodegradable	OTFTs	[64]
			DMSO swelled	Filtration method	5.7	127 MPa	Only biodegradable	PHOLED	[65]
			Surface acetylation with acetic anhydride	Dipping method	NA	NA	Only biodegradable	Substrate only	[66]
			Surface acylation with lauroyl chloride	Dipping method	5.0 ± 0.7 nm	NA	Only biodegradable	Substrate only	[67]
			Reduced graphene oxide	Layer-by-layer assembly	3.5~4.2 nm	11.7 MPa	Only biodegradable	Supercapacitor	[68]
	NO	NO	Blend with CNTs	Filtration method	NA	142-225 MPa	None	Substrate only	[69]
Cellulose nanofibers composites	YES	NO	Composite with cellulose ether	--	NA	Up to 30 MPa	Only biodegradable	OPVs	[70]
			TEMPO-oxidised nanofibers - hydrophobized via silanization	Dipping method	NA	100 MPa	None	Silicon solar cells	[71]
			Micro-fibrillated cellulose with Kaolin and precipitated calcium carbonate	Filtration method Supercalendering	0.3–0.5 μm	NA	Only biodegradable	Printed silver nanoparticles circuits	[72]

			Composite with polydopamine	Filtration and pressing method		106.5 MPa	Only biodegradable	Substrate only	[73]
Regenerated cellulose films	YES[g]	NO	Spin cast trimethylsilyl-functionalized microcrystalline cellulose (TMSC)	Acid removal of silane group	3.9 nm	NA	Only biodegradable	OFET	[74]

[a] Surface roughness of several commercial papers is in the range 5 ÷ 10 μm.[54] [b] Strain resistance of commercial paper ~2.5%. [c] SC = solar cell; FET= field effect transistor; OFET= organic field effect transistor; P3HT= poly(3-hexylthiophene); PCBM = [6,6]-phenyl C_{61} butyric acid methyl ester; OPV= organic photovoltaics; OLED= organic light emitting diode; OTFT= organic thin film transistor; PHOLED= phosphorescent organic light emitting diode; [d] Optical transmittance and transmittance haze > 80%. [e] Optical transparency ~96% and transmittance haze ~60%. [f] Typically, nanopaper presents high optical transparency and transmittance haze. The paper by Yano et al. [51] reports an optical transparency ~72% at 600 nm. [g] Transmittance in the visible region > 90%.

Many types of commercial paper typically display a surface roughness of the order of few to several μm, while commercial PET or PEN substrates, that represent a benchmark as substrates for printed electronics, present much lower surface roughness, of the order of few to several nm. Mechanical treatments like supercalendaring, applied in combination with specific coatings, are a successful approach to electronic paper.[4] Supercalendaring can produce a finely glossy paper, but it has high operation costs. However, this is still considered compatible with the economic and environmental advantages to produce paper electronics, at the point that specialty papers are already present on the market with the specific application as substrates for printed electronics. Typically, they have multiple coatings, high surface smoothness, reduced water permeation and non-fouling surface, and they are compatible with clean room operational condition and thermal treatments.

However, electronic products obtained using this kind of substrate still have to be released on the market. For instance the completely biodegradable and recyclable PowerCoat is compatible with thermal metal evaporation (**Figure 1**a), thanks to its surface smoothness, [37] while thermal evaporation of a thin Cu electrode was unsuccessful on rough paper.[35]

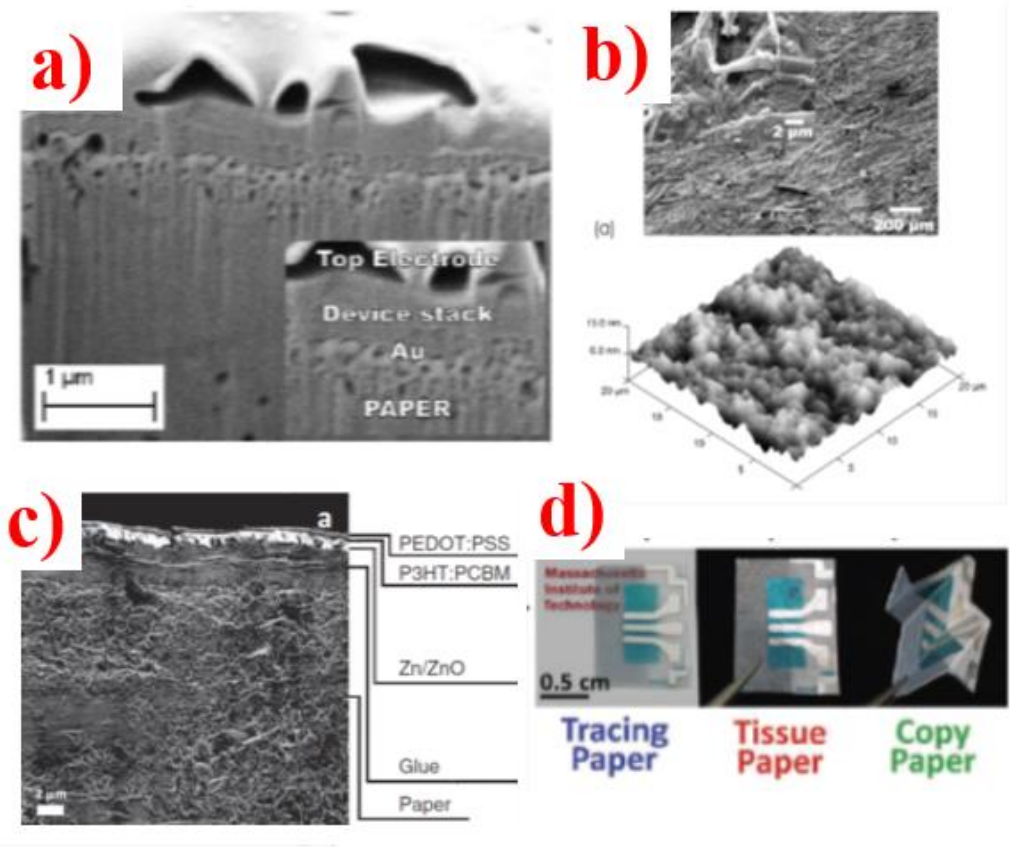

Figure 1. a) Cross section SEM image of a SEM image of the cross-section of a perovskite SC deposited on commercial electronic paper. Reproduced with permission;[37] Copyright 2017, IEEE. b) Top: SEM Micrograph of newspaper before the treatment. Bottom: AFM topography of the same paper after parylene and ORMOCER treatment. Reproduced with permission;[42] Copyright 2005, John Wiley and Sons. c) SEM image of an OPV cross-section. The paper/glue/ZnO/Zn/ZnO/P3HT:PCBM/PEDOT:PSS. Zn/ZnO layers are not distinguishable. Reproduced with permission.[9] Copyright 2011, John Wiley and Sons. d) PEDOT:PSS PVs printed by organic chemical vapour deposition (oCVD) on as-purchased tracing paper (~ 40 µm thick), copy paper(~ 120 µm thick), and tissue paper (~ 40 µm thick). Reproduced with permission.[50] Copyright 2015, John Wiley and Sons.

A substrate for electronic devices deposition was attained from newspaper by polymer coating. The coating was produced evaporating parylene dimer that was then oxidatively polymerized on the newspaper surface to constitute a barrier layer. Thereafter, a smoothing layer was spin-

cast, based on a silicate inorganic–organic hybrid polymeric material, named ORMOCER. The smoothed newspaper was compatible with deposition of a thermally evaporated bilayer photodiode.[42] The Figure 1b shows the SEM micrographs of the starting paper and the final smoothed morphology of paper after the treatments.

Another strategy consists in gluing a conductive cathode on commercial paper. The layer is transferred from commercial Zn-metallized polypropylene (PP) foils and PP is removed after the transfer. Exposure of the Zn layer in air produces a surface ZnO hole blocking and oxygen barrier layer (Figure 1c). It is possible to pattern paper surface with a cyanoacrylate glue applied by gravure printing before transferring the cathode[9] or to fully cover paper with the Zn/ZnO layer, by gluing the PP side on it. With this second approach, the PP smoothens paper surface and works as a protective layer for the next deposition of active inks.[35]

Covering different kinds of common paper with a transparent anode without previous smoothing treatment is also possible by using PEDOT:PSS (Figure 1d).[50] Deposition is performed by simultaneous exposure to vapor-phase monomer (EDOT) and oxidant ($FeCl_3$) at low substrate temperatures (<100 °C) and moderate vacuum (~ 0.1 Torr). *In situ* shadow masking helps to create well defined polymer patterns on paper surface. The evaporated PEDOT:PSS displays mechanical robustness, with unaffected conductivity by several compressive flexing cycles at 5 nm radius.

A pivotal optical property of paper is opacity, essential for reading documents since it avoids interference from print images on the back side of a page. The opacity is a consequence of light scattering in many directions produced by the rough paper surface. However, optical transparency may be a desired property for specific applications: it would enable technological applications in smart windows and smart packaging, and illumination from both sides for light responsive devices such as photodiodes and photovoltaic cells.

Infiltration of a transparent plastic, like an epoxy resin, into standard paper pores can increase transparency. The process can be potentially implemented in a roll-to-roll machine for large scale production.[20] The new plastic-paper material possesses a high optical transmittance (> 85%) and a high transmittance haze (> 90%; i.e. ratio between diffused and total light intensity) in a broadband wavelength, enabling enhancement of light coupling through the substrate (**Figure** 2a). Other approaches based on the same concept are: infiltration of an ionic gel ink, that also confers conductivity to the resulting ionic gel paper,[41] infiltration of carboxymethyl cellulose (CMC),[49] or top coating with green polymerizable deep eutectic solvent (PDES).[40]

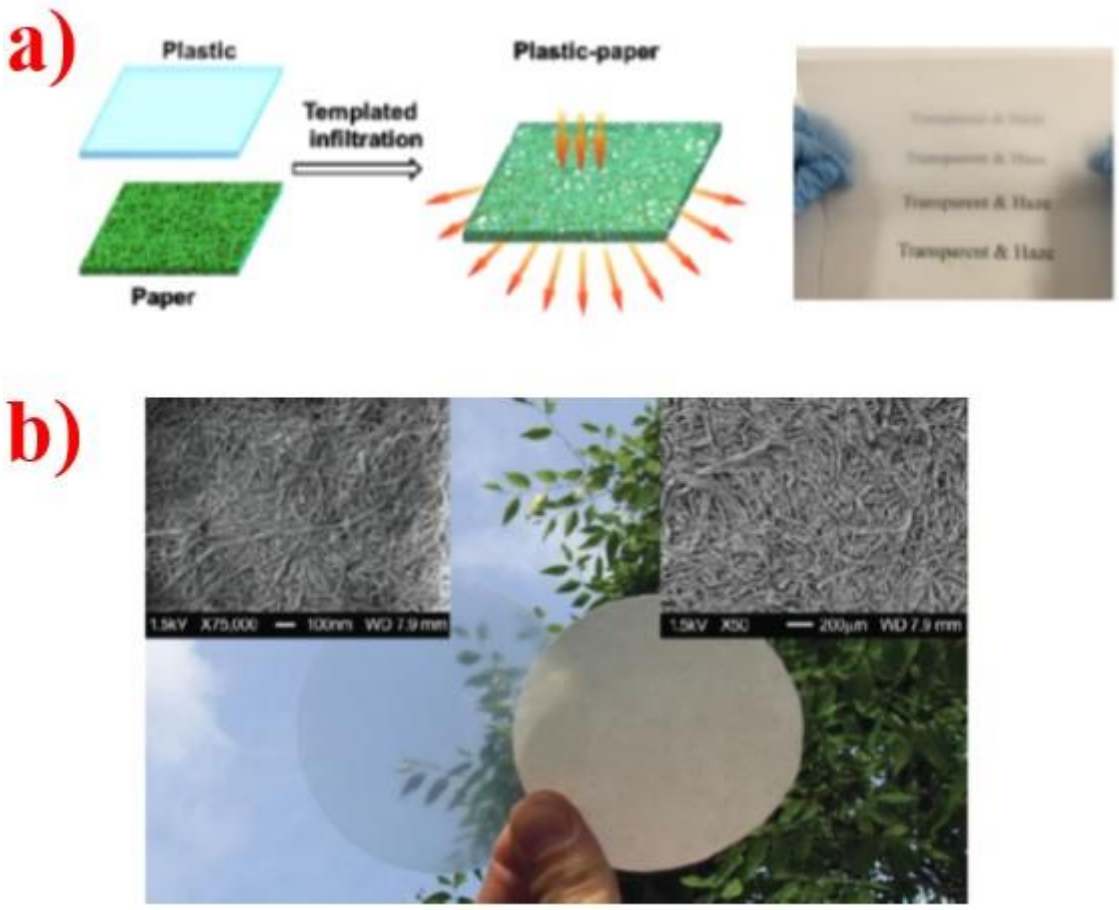

Figure 2 a) Concept of plastic-paper production and a photography of the transparency&haze effect. Reproduced with permission.[20] Copyright 2012, Royal Society of Chemistry. b) Nanopaper (left) and paper (right). Optically transparent paper (left) is composed by 150 nm cellulose nanofibers. The upper left inset, with a scale bar of 100 nm, shows a SEM micrograph

of the surface of transparent nanopaper. Conventional cellulose paper (right) is composed by 30 μm pulp fibres. The upper right inset, with a scale bar of 200 μm, shows the SEM micrograph of the surface of a sample of filter paper. Reproduced with permission.[55] Copyright 2009, John Wiley and Sons.

Another route to transparency is given by transparent all-cellulose composites. The fibres are selectively dissolved and swelled by dipping them in a solvent and then re-gathered by compression and drying. This method was applied to filter paper by using N,N-dimethylacetamide as solvent containing LiCl;[52] an alternative is represented by processing the fibres by TEMPO/ NaBr/NaClO oxidation to introduce carboxyl groups onto the cellulose. This weakens the hydrogen bonds between the cellulose fibrils and causes the wood fibres to swell up and collapse resulting in a high packing density and excellent optical properties. The TEMPO oxidised paper can be used as light harvesting enhancing coating in an OPV solar cell.[51]

A striking innovation is given by the use of transparent nanopaper.[55] Nanopaper is composed of nano-dimensioned cellulose crystals and presents high haze and transparency, thanks to the reduced dimension of interstices among nanofibers. The Figure 2b) shows the typical appearance and morphology of filter paper and nanopaper, obtained from 150 nm cellulose nanocrystals (CNCs). The preparation of good quality nanopaper requires procedures taken from the paper industry, including mechanical compression under vacuum and pressures. Nanopaper usually does not need coating layers to be compatible with electronic inks deposition. Some examples of organic and perovskite solar cells deposited on cellulose nanopaper, obtained from tiny nanocrystals or longer (1-2 μm) nanofibres, have already appeared on the literature.[56,57,59,61,63,64]

Even if nanopaper possesses more appealing optical, mechanical and thermal properties than PET,[19] it still has high costs (0.7-7$ g^{-1}, though it has lower grammage than conventional paper)[75] and is not commercialized, yet; it is mechanically more resistant than standard paper[58] but displays some issues relevant to its highly hygroscopic nature: it swells in water,[61] so it needs some protective treatments to improve its durability in time. Many recent studies have faced the problem proposing protocols for increasing nanopaper stability[65] by hydrophobization [66,67,76] or amphiphobization,[53] or through the formation of crystalline cellulose nanocomposites with cellulose ethers.[70] Some of the strategies were successful and had the potentiality to be applied on large scale production. One limiting aspect connected to the nanopaper or CNCs involvement in new technologies is however still due to the commercial availability of nanofibers and nanocrystals with different length and characteristics, which is, at the moment, still limited.

2.2 Energy storage devices

The characteristic of paper that is considered as a drawback for its implementation in thin film devices, i.e. the rough surface, may represent a desired property in energy storage devices. Paper fibres have up to several tens of μm length and 20 μm width, and form pores with micro-dimensioned diameter. In energy storage devices paper should act as a flexible and conductive substrate that works as a current collector. Moving in this direction, and conversely from what observed in thin films solar cells, the high porosity enables to exploit the capillary action to absorb active electrode materials. Indeed, the goal here is to get a highly conductive paper that is flexible, mechanically resistant, and highly accessible to ions in the electrolyte. For this goal different approaches have been pursued,[77] mainly based on functionalization with single walled carbon nanotubes (SWCNT) or silver nanowires, [48] graphene,[54] nanoparticles,[43] etc. The characteristic of these coatings lays in their feature to completely cover the cellulose fibres and electrically connect neighbour fibres. This is clearly shown in the **Figure** 3a-b), for the case

of SWCNT: nanotubes are highly conductive and flexible, and they can associate strongly with the cellulose surface and electrically bridge fibres.[48] The final electrode is flexible and it can be prepared by treating the paper with a SWCNT solution. The Figure 3c-d) shows a photography of a SWCNT conductive paper, which is proposed as lightweight and flexible electrode for flexible storage devices in place of a copper foil.[77]

In order to further increase the potential storage of ions/charges it is necessary to increase the surface area. Cellulose nanofibrils networks are ideal nanoporous materials with extremely high content of surface hydroxyl groups that potentially enhances their attitude to self-assembly with the conductive inks. Indeed, a recent work has demonstrated spontaneous association into aggregates of cellulose nanofibers and carbon nanotubes (CNTs) and, more in general, carbon nanomaterials. The close affinity of the two materials allowed the preparation of black CNT-nanopaper, displayed in the Figure 3e).[69] Optical transparency has also been demonstrated for supercapacitors, using nanopaper as substrate. In this case, the transparent reduced graphene oxide (RGO) is used in place of CNTs to enable charge storage: co-deposition of RGO and cellulose nanofibers is allowed by layer-by-layer wet method performed under the assistance of divalent metal ions. Thanks to the close interaction with the cellulose nanofibers, RGO aggregation can be prevented, maximising their potential to store charges.[68]

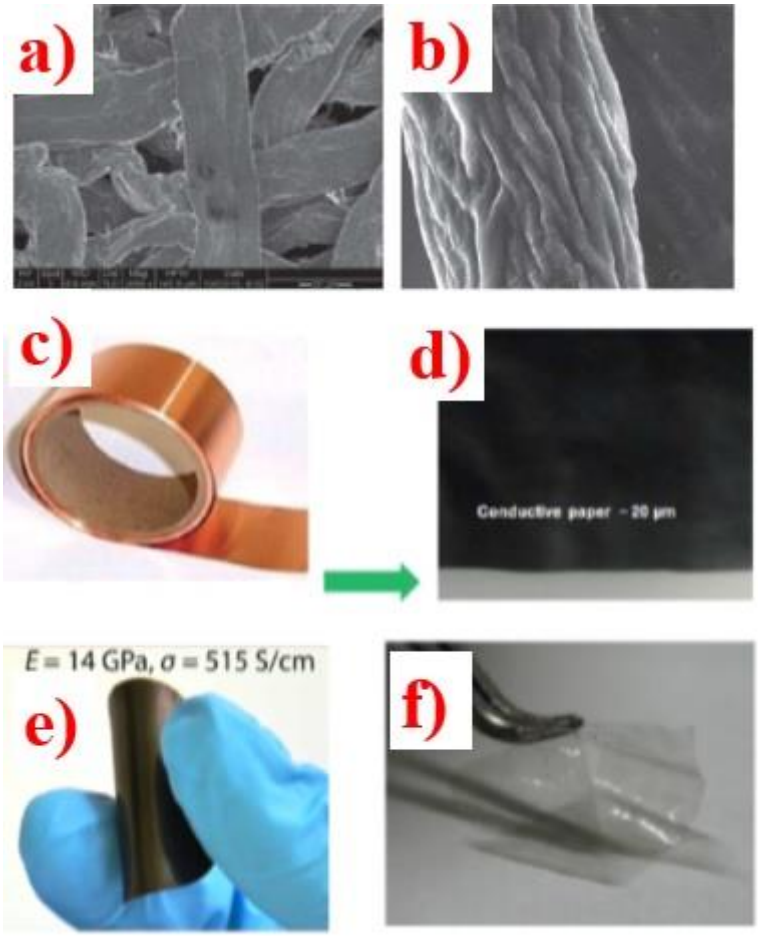

Figure 3. a) SEM micrograph of the SWCNT-conductive paper. The SWNTs are flexible, and adhere to the fibres surface, eventually bridging over the gaps between paper fibers. b) Higher magnification SEM image revealing the presence of SWCNTs on the fibres surface. Reproduced with permission.[48] Copyright 2009, National Academy of Sciences. c,d) The perspective of replacing thin film conductors, like heavy metal foil, i.e. Cu foil, with conductive paper (d). Reproduced with permission.[77] Copyright 2012, Royal Society of Chemistry. e) CNT functionalized nanopaper. Reproduced with permission.[69] Copyright 2017, American Chemical Society. f) Flexible reduced graphene oxide (RGO)- nanopaper. Reproduced with permission.[68] Copyright 2013, Royal Society of Chemistry.

3. Printing technologies for paper electronics

Traditionally, the invention of the printing press is ascribed to Gutenberg in the 15th century. This consisted in the flat-bed type, whilst the rotary one came about in the 19th century. The main medium on which inks were transferred to via printing presses was paper. Printed electronics has been a much more recent development arising mainly towards the end of the 20th century. The main substrates for printed electronics have historically consisted in glass, plastic sheets and metal foils. The development of paper electronics, has seen a surge in interest by research laboratories in more recent years, bringing together the three key fields of "printing", "paper and "electronics" at the same time. Current deposition techniques for device manufacturing on paper substrates consist mostly of those already utilized for solution processing of these layers on more conventional flexible substrates either for PV,[31,75,78,79] batteries [18,32,33,80,81], supercapacitors, [34] or conductive and semiconducting materials.[82–85]

However, as detailed in Section 2, in the case of light harvesting devices, an overlayer or treatment is usually applied over the surface of paper to improve planarity and printing capabilities of its surface.[11,34] Ink formulation may also be optimized according to the different wetting and adhesion properties of the papers substrates. Differently, the porosity of fibre-based cellulosic substrates may instead be beneficial and exploited for the manufacture of for some types of storage devices as described below.

Currently, spin coating (high control over film thickness but high material waste) still represents the main liquid solution deposition technique utilized in over 50% of the works reviewed in Section 4 for PV devices on paper. Drop casting is also frequently used to deposit active inks on paper substrates, typically when thicker films are required or when wetting issues arise during spin coating. However, drop casting has the drawback of offering very poor control on film thickness. These two techniques are not applicable to high-throughput roll-to-roll industrial scale manufacturing. Interestingly, around 1 in 6 works in the literature employed doctor blade, which is the first step for a more scalable coating, especially when converting this technique in

its more sophisticated slot-die form for future industrialization. Slot die coating is a technique where ink is made to go through the interspace in a steel body distributing the ink uniformly over the underlying substrate relatively to which is moved. Respect to doctor blade, it is a technique which gives the possibility of controlling with higher precision the amount of ink used (and wasted) and of obtaining a rectangular patterned film. The rectangular form covers most shapes used in either PV, battery or super-capacitor applications. Other scalable techniques which have been employed for developing PV on paper (see section 4) consisted in screen printing (a non-contact printing technique where the material to be applied is squeezed through a pre-patterned screen mainly used for depositing thicker films, i.e. $5{\cdot}10^{-1}$ - $5{\cdot}10^{1}$ μm), and flexographic printing (where the ink is transferred from a protruding relief on a printing roll, made of rubber or a photopolymer).[75,86] The utilization of spin coating or drop casting for PV cells for the majority of the works published in the literature to date, with no reports on techniques such as slot die or inkjet printing, represents a strong indication that the development of printed solar cells on paper is still well in its infancy along its technology roadmap.

In the case of batteries and supercapacitors (see Section 5), the main means of deposition that have been utilized have been screen printing, and inkjet printing. In general, these are similar to those used for printing PV devices, except for techniques such as impregnation, vacuum filtration and Meyer rod coating. This latter technique is based on the use of a stainless steel rod, wound tightly with a stainless steel wire which is used to doctor off the excess of the coating solution and to control the coating thickness. Stencil printing consists in spreading a paste uniformly over a surface except where stencils block this transfer (i.e they act as masks as well as spacers that determine film thickness). Stencils are made of materials such as metals. These printing techniques are typically used to deposit the electrodes and the electrolyte. It is interesting to point out that the textured and porous consistency of cellulose paper enables the creation also of 3-D electrode systems supported by the substrate. In this case, the conductive

materials are embedded in the paper substrates, rather than forming separate layers deposited on their surface. Especially in cases where large thicknesses can be beneficial (e.g. increasing electrodes conductivity or capability to store charges), this strategy has been applied either via soaking, *in situ* polymerization or vacuum filtration for the manufacture of flexible energy storage devices.[34] The former technique consists in soaking the rough paper substrate in a monomer and carrying out subsequent polymerization (e.g. of a conducting polymer like PANI and PPy). Both the exterior and interior of cellulose fibres become coated with material at the end of the procedure.[34,87] Vacuum filtration is a popular technique for making electrodes rapidly for storage devices and consists in using paper as a "filter" to block materials/particles with sizes larger than the pore size of the paper substrate, exploiting paper's own intrinsic 3D porous structure.[34] At the end of the process of filtration of the solution containing the material to be deposited (passage of the solution is generally generated by difference in pressure, i.e. vacuum), the surface of fibres and the pores will have been coated with the solid content of the material. The vacuum filtration method has often been used to prepare carbon based (e.g., graphene, graphite, CNT) paper-based electrodes. The challenge for these deposition methods, in which the substrate becomes the electrode, is to be able, at the industrial scale, to generate patterns on a larger paper substrate when wanting to monolithically integrate these with other electronic or non-electronic components. The alternative would be to laminate the devices after their fabrication.

Table 2. Comparison of different large area deposition techniques for printing layers for PV and energy storage device from inks or pastes. Data collected from references [31–34,83,88] **and the authors' experience.**

Fabrication technique	R2R compatible	Material waste	Layer thickness accuracy	Average Layer thickness (μm)
Spin coating	N	very high	very good	10^{-2} - $5{\cdot}10^{-1}$

Blade coating	Y	moderate	good	10^{-1} - $5{\cdot}10^{0}$
Slot die coating	Y	low	very good	10^{-2} - 10^{0}
Spray coating	Y	moderate/high	low	10^{-1} - 10^{4}
Screen printing	Y	low	moderate	$5{\cdot}10^{-1}$ - $5{\cdot}10^{1}$
InkJet printing	y	low	good	10^{-2} - $5{\cdot}10^{-1}$
Flexographic printing	Y	low	moderate	10^{-2} - 10^{0}
Gravure printing	y	low	good	10^{-2} - 10^{0}
Dispenser printing	Y	low	moderate	$5{\cdot}10^{-1}$ - $5{\cdot}10^{2}$
Stencil Printing	Y	moderate	moderate	10^{0} – 10^{2}
Mayer rod printing	Y	low	moderate	10^{0} – 10^{2}
Soaking and polymerization	?	moderate	low	high-depending on substrate and texture
Vacuum filtration	?	moderate	Low	High-depending on substrate and texture

It can be noted that all the techniques reported in **Table 2,** except for spin, blade coating, Mayer rod printing, soaking and vacuum filtration, guarantee a print resolution[83] at least in the range of 100-200 microns which is satisfactory for the relatively large-area of the devices covered in this review (i.e. PV and energy storage devices). Rather than printing the films directly in their final form, patterning can occur after coating or deposition of the films. Whereas mechanical scribing is also applicable, laser patterning has become an important tool in the industry of thin film optoelectronics[89] assuring scribing widths below the 100 μm range consistently. Scribing by raster scanning laser beam systems thus guarantee a more effective use of space minimizing the dead areas of the devices. Whereas lasers are routinely used when fabricating PV modules on glass and even on PET,[90] application and optimization of its parameters such as wavelength, power, pulse duration, fluence, repetition rates, for patterning printed PV cells on paper requires investigating.

The successful application of large area printing techniques to light harvesting and storage devices not only will enable a seamless integration of these two types of symbiotic devices

monolithically on the same substrate, but also the possibility of applying these with other types of printed optoelectronic devices (e.g. transistors, sensors, displays) for the development of paper electronics of the future. As one of the major benefits of paper is its cost, the opportunity of printing electronic devices, rather than utilizing other techniques, can make printed electronics an enabling technology for paper-based applications.

4. Printed Photovoltaic technologies on paper.

In this section, we review the developments of solar cells on paper substrates. We will start by analyzing a critical issue, that of producing effective electrodes, one of which needs to be transparent. We will then cover the literature on the different photovoltaic technologies fabricated on paper in which at least one of the layers has been solution processed. We will conclude this section by describing issues for future development.

4.1. Electrodes

Solar cells are fabricated between two electrodes: i.e. a transparent/window and a back electrode. Commonly used materials for window electrodes are based on transparent conductive oxides (TCO), such as fluorine-doped tin oxide (FTO), indium tin oxide (ITO), indium zinc oxide (IZO), or aluminium-doped zinc oxide (AZO), although in some cases the TCO is replaced by metal grids, metal nanowires, conductive polymers (i.e PEDOT:PSS), carbon nanotubes, 2D materials such as graphene, multilayer stacks of thin metal/dielectrics and a combination of these. [37,91–97] The back electrode usually consists of a thin metallic film i.e. gold (Au), silver (Ag), aluminium (Al) or Platinum (Pt). Most of the solar cells are directly fabricated on a glass/plastic substrate covered with a TCO and the back electrode is deposited on top of the solar cell stack; alternatively, when metal foils are used as substrates[79,98] the window electrode is deposited as the last constituent layer of solar cell. Additionally, the polarity of transparent and back electrode (cathode or anode) can vary depending on the solar

cell architecture (i.e direct or inverted, or p-i-n or n-i-p). In order to avoid any confusion and provide a comprehensive overview, we will define bottom and top electrode as the electrode deposited on the substrate or the last layer, respectively, regardless of their transparency or polarity.

As already reported in Section 2, the main challenge in the fabrication of paper based solar cell is the deposition of the bottom electrode on cellulose due to roughness and porosity. [9,59,63,99–101] In order to produce successful devices deposited on paper, the first active layer, the bottom electrode, needs to be a high quality homogeneous, thin and crack -free layer. Researchers implemented four different methods to deposit bottom electrodes on rough substrates: 1) Optimization of bottom electrode deposition avoiding or exploiting the surface structure,[50,102–104] 2) modification of the paper surface by using planarization layers,[42,99] 3) use of nanocellulose substrate with smooth surface,[70,101] and 4) development of conductive cellulose substrates.[63] Once the bottom electrode is successfully deposited, the electron/hole transport, active and hole/electron transport layers are deposited following the same procedures used in the control/reference cells on glass or plastic substrates. Finally, the top electrode is mostly deposited by metal evaporation,[35,37] although lamination[62] and sputtering deposition[46,56] are also used.

4.1.1. Transparent electrodes

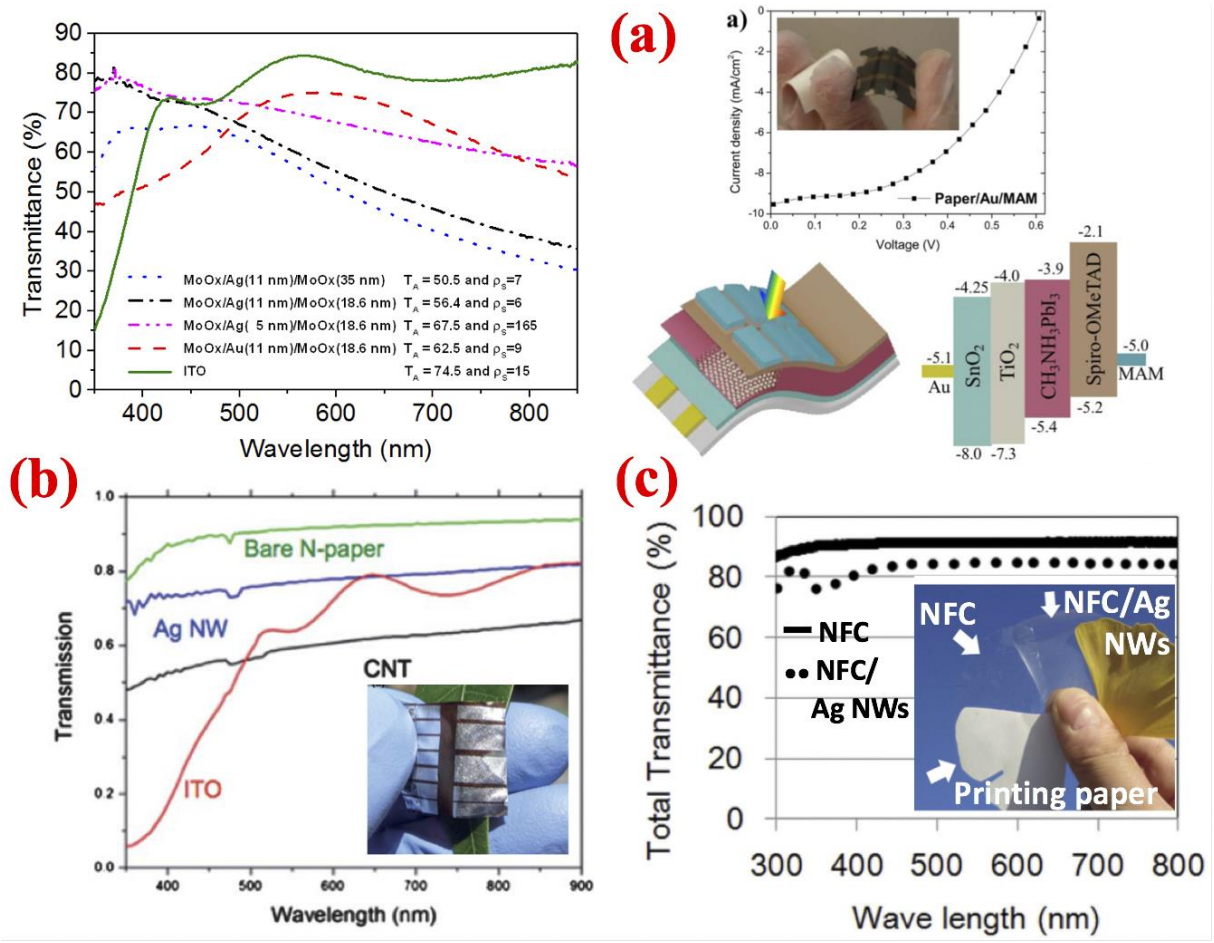

Figure 4. Transmittance spectra of transparent (window) electrodes implemented in solar cells on cellulose paper substrates. (a) On the left, thickness optimization of evaporated MoO_x/Metal/MoO_x on PET, with inset data representing the average transmittance T_A [%] in the 350-850 nm wavelength range and the sheet resistance ρ_s [Ω/□]; on the right, schematic architecture, energy level diagram, and characteristic J-V curve, with inset picture of a complete device on opaque paper, fabricated with a MoO_x/Au/MoO_x transparent top electrode. Reproduced with permission.[37] Copyright 2017, IEEE. (b) Nanopaper covered with sputtered ITO, or printed carbon nanotubes (CNT) or Ag nanowires (AgNWs); an organic solar cell, shown in the inset photograph, was fabricated on top of the nanopaper/ITO substrate (bottom electrode) Reproduced with permission.[56] Copyright 2012, Royal Society of Chemistry. (c) Pristine nanofibrillated cellulose (NFC) paper (solid line), and conductive NFC paper (dotted line) obtained by inclusion of AgNWs; the NFC/AgNWs electrode was used as bottom

electrode of an organic solar cell ; in the inset, photograph of white opaque printing paper, non conductive NFC and conductive NFC/AgNWs paper substrates Reproduced with permission.[63] Copyright 2015, Nature.

Depending on the cellulose substrate, the transparent (window) electrode is deposited either as bottom or top electrode. Nanocellulose paper allowed the deposition of window electrode without any need of surface treatment thanks to its optical transparency and smooth surface;[70] conversely, in case of an opaque paper substrate the window electrode is deposited on top of the solar cell stack. TCOs including ITO and IZO presented several optical and electrical advantages and have been therefore widely used in paper solar cells.[4,56,70,99,101] ITO is deposited by sputtering in an Argon atmosphere with a high-purity In_2O_3:SnO_2 target. To enhance the electron/hole extraction, a semiconductor buffer layer (i.e ZnO[101]**)** is coated between the ITO electrode and active layer. A sputtered ITO electrode was compared with printed silver nanowires (AgNWs) and carbon nanotubes (CNT), as shown in **Figure** 4b).[56] At 550 nm, ITO delivered a better transmittance:resistivity combination (65%:12Ω/□) than CNTs (60%:200Ω/□) and AgNWs (78%:25Ω/□).

Another transparent electrode commonly used for fabricating solar cells on paper is the dielectric-metal-dielectric (DMD) electrode, consisting in a thin layer of metal sandwiched between two semiconductor oxides. Dielectric layers act as both seeding layers for metal film[37] and as anti-reflection films.[35] The thickness of the metal and its growth (morphology) define the transparency and conductivity of the electrode.[37,57,105] Both n-type and p-type DMD electrodes have been integrated in paper solar cells. N-type (i.e. those that extract electrons) DMD electrodes such as TiO_x(40nm)/Ag(10 nm)/TiO_x(40nm)[57] or ZnO(40nm)/Ag(12nm)/ZnO(40nm)[106] had a resistance:trasmittance ratio of only 2Ω/□:70% (when measured between 400-600 nm) or 7.2Ω/□:81.7% (when measured between 400–

800nm), respectively. TiO_x/Ag/TiO_x electrode was used as bottom window electrode on nanopaper for perovskite solar cells (PSC) while ZnO/Ag/ZnO was successfully implemented in organic solar cell. Similarly, p-type DMD presented a good relation between transmittance and sheet resistance. Leonat et al.[35] optimized a MoO_3(8nm)/Ag(13nm)/MoO_3(25nm) electrode obtaining a sheet resistance of ~5 Ω/□; likewise, Castro-Hermosa et al.[37] studied MoO_x/Metal/MoO_x electrodes for paper perovskite solar cells, the transmittance spectra of which are shown in Figure 4.a. Although silver increased the conductivity of the electrode, it also allowed UV (wavelength less than 400 nm) transmission which can lead to perovskite degradation[107] as well as possible issues of Ag interacting directly with the perovskite via diffusion or pinholes. On the other hand, the more stable gold increased the electrode transmittance by 10% in relative terms (from 56.4% to 62.5%). Therefore, the final optimized electrode stack consisted of MoOx (17.5nm)/Au(11nm) /MoOx (18.6nm) with T_A = 62.5% and ρs = 9Ω/□.

A less complex transparent electrode is represented by semi-transparent metal thin films (<25 nm) on their own; however, the solar cell performance is restricted by metal transmittance. [42,59,61,108] Costa et al.[59] deposited 20 nm of Ag on Nano-Crystalline Cellulose (CNC) and **N**anoFibrillated Cellulose **(**NFC) substrates. Organic solar cell (substrate/Ag/ZnO:Al/PFDTBTP:PC70BM/MoO_3/Ag) performance depended on substrate morphology and was lower on NFC than CNC because the higher roughness of NFC induced high series resistance. Additionally, the introduction of a buffer layer as polyethylenimine (PEI) on to the ZnO:Al mixture film led to a reduction of surface roughness and tuned the electrode work function from 4.41 eV to 4.28eV. In a similar work, Zhou et al. [61] modified the Ag surface with a ethoxylated polyethylenimine (PEIE) buffer layer improving the Ag conductivity. Additionally, a transfer lamination of semi-transparent PEDOT:PSS top hole-collecting electrode was developed by Zhou et al. [62] (See **Figure** 5d). First, PEDOT:PSS (PH1000 with 5 wt% DMSO) was deposited on a PDMS substrate by spin coating (1000 rpm for 30 s) and

dried at room temperature for 10 min. Then, the electrode was mechanically sized and transferred on top of the active layer (P3HT:ICBA). Finally, the PDMS was removed. This approach represents a simple vacuum-free deposition process for transparent top electrodes and was necessary to protect the underlying nanopaper substrate and device layers from water solvent, used for PEDOT:PSS deposition. La Notte et al.[109] used a sprayed modified PEDOT:PSS as conductive glue for the application of a composite cellulose/graphene nanoplatelets electrode.[109] Moreover, Barr et al.[50] fabricated a 250-cells organic module presented in Figure 5a) where PEDOT was deposited by vapour printing. The oxidative chemical vapour deposition (oCVD) allowed large area deposition, pattern design and thickness control on any surface including rough and hydrophobic paper. PEDOT:PSS has also been incorporated as top electrode by flexographic printing (Figure 5b).[9] Furthermore, Nogi et al.[63] incorporated the conductive transparent electrode within nanocellulose paper (Figure 4.c). AgNWs (Diameter=50–100 nm, Length=5–10 μm) were incorporated into nanocellulose using three different methods: bar-coating followed by heating or mechanical pressing and drop-casting. The transmittance of the conductive and pristine paper is presented in Figure 4c): paper achieved a favourable transmittance:resistance combination of T_A = 91% (at 600nm) and ρs = 34Ω/□.

4.1.2. Opaque electrodes

An opaque metal electrode is often deposited on opaque cellulose paper as bottom electrode while on transparent cellulose substrates the opaque back electrode is deposited on top of the device. The most used opaque top electrodes are: MoO_3(8-15 nm)/Ag (100-150 nm),[59,61,70] Ca(7nm)/Al(200nm)[56]or Au (80-120nm).[46,57] Metal electrodes provide chemical stability,[37] low cost deposition,[9,35,102,104] light scattering,[110] and high conductivity.[111] Voggu et al.[101] used gold (80nm) as bottom electrode on different commercial papers including standard office

paper, photography paper, wax paper and parafilm. With the addition of a chromium (10nm) seeding layer, the growth of gold was enhanced. SEM images of electrodes showed high porosity and discontinuities due to the roughness of paper, and bad adhesion on photography paper was also noted. Then, authors selected a smooth bacterial nanocellulose substrate to prevent interference from these defects in the deposition of gold. Alternatively, several authors reported the use of planarizing layers before metal deposition, in order to decrease the porosity and roughness of cellulose substrates.[42,99] Nevertheless, gold electrodes can present particle-aggregation, which produce rough films.[46] Other metals including thermally evaporated silver,[4,62] solution processed nickel[102,111] and laminated zinc[9,35] have been used in paper solar cells. Hubler et al.[9] reported a roll-to-roll (R2R) printed organic solar cell on the paper substrate described in the Figure 1c), prepared by gravure printing/gluing a zinc foil. The Figure 5b) shows the system of rollers used to modify paper and to glue the zinc foil on it. Gravure printing of glue allowed a selective deposition (patterning) of zinc foil though it and it also could be wet etched with acetic acid.[35] The Zn electrode had ohmic behaviour, a work function of 4.3 eV, low surface roughness (80 nm) and it was deposited in air with a low-cost process. Nickel electrodes deposited by chemical bath reaction at low temperature on paper substrate were used in dye-sensitized solar cell (DSSC) fabrication.[102,111] Nickel electrodes presented better chemical stability than gold when it was immersed in the electrolyte.[102] Characterization of Ni films evidenced a uniform deposition (SEM microscopy) and low resistance (< 1 Ω/□, four point probe), which increased when the electrode was annealed.[111] However, metals such as gold,[35] silver and zinc are very hydrophobic[112,113] and lead to poor coverage and inhomogeneous film deposition which would be problematic for the fabrication of printed solar cells. This problem is generally solved with application of UV-ozone surface treatment,[114] use of buffer layers such as polyethylenimine (PEI)[62] or ethoxylated polyethylenimine (PEIE),[35] or metal surface passivation with natives oxides such as ZnO on Zn foil.[9,35]

Conductive polymers are a suitable alternative to metal back electrodes for paper solar cells. Poly(3,4-ethylenedioxythiophene): poly(styrenesulfonate) or PEDOT:PSS is widely applied in optoelectronics since it provides satisfactory transmittance and resistance (especially in the vertical direction) behaviour (i.e transmittance:resistivity combination of 85%:25Ω/□[115]) and a high work function (useful for the extraction of holes).[116] Moreover, it is solution processable at low temperatures, therefore compatible with R2R printing techniques and paper substrates. For example, PEDOT:PSS doped with dimethylsulfoxide (DMSO) was drop cast on paper resulting in a homogeneous deposition which was independent of substrate hydrophobicity and roughness.[108] Also, Lee et al.[100] coated a commercial A4 paper by immersion in a mixed solution of graphene dots (GD) and PEDOT:PSS (1:1). The resulting electrode was compared with a sputtered Pt electrode as a counter electrode for DSSC (dye-sensitized solar cells), showing an improvement by a factor of 2.9. The incorporation of graphene dots determined a 6-fold increase in conductivity compared to a PEDOT:PSS only electrode. GD:PEDOT:PSS paper electrodes also presented lower resistance and higher flexibility compared to Pt coated cellulose.[100] Anothumakkool et al.[117] reported a PEDOT:PSS electrode deposited using immersion technique. The high conductivity of the electrode (Rs = 4 Ω/□) was attributed to the multi-layer structure of PEDOT. Additionally, the PEDOT electrode was stable for 40 days in air. Besides that, Dasari et al.[104] fabricated a multilayered graphene (MuLG) electrode via a simple H2B pencil scribing. The electrode presented high resistance (5kΩ/cm^2) and high roughness. Planarization was achieved by depositing a PEDOT:PSS layer on the surface. Finally, Gao et al. [118] screen printed a carbon electrode (150 um) on cellulose paper exhibiting high roughness and sheet resistance 43 Ω/□ when measured with four-point probe. Roughness was decreased with a polished process which enhanced the conductivity of electrode reducing the electrode resistance to 14.2 Ω/□.

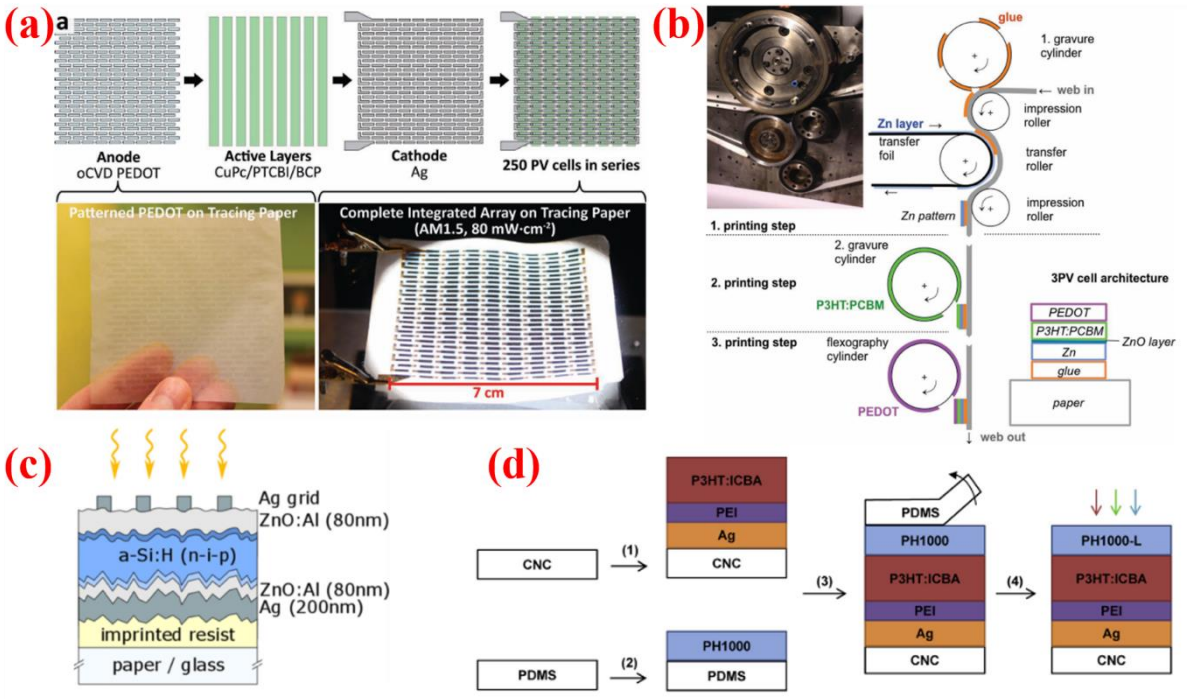

Figure 5 Deposition of bottom electrode (a-d) on cellulose paper using different deposition techniques. (a) Oxidative chemical vapour deposition (oCVD) of PEDOT grid on tracing paper. Organic solar module contained 250 cells. Reproduced with permission.[50] Copyright 2011, John Wiley and Sons. (b) Roll-to-roll (R2R) lamination of Zn electrode on glossy paper, gravure printing of P3HT:PCBM active layer, and flexography of conductive PEDOT top electrode. Reproduced with permission.[9] Copyright 2011, John Wiley and Sons. (c) Paper surface modification with an UV resistive resin. Resin allowed a controllable design of surface pattern which enhanced the light scattering in an a-Si solar cell. Reproduced with permission.[110] Copyright 2017, John Wiley and Sons. (d) Transfer lamination of PEDOT:PSS top electrode. Reproduced with permission.[62] Copyright 2013, Elsevier B.V. All rights reserved.

4.2. Photovoltaic technologies

Photovoltaics can be divided into three main categories: first, second and new generation solar cells.[119] First generation PV is based on mono- and multi-crystalline silicon solar cells, mature

technologies with large scale production, that in 2017 accounted for 93.0% of the global annual PV power production.[120] Crystalline silicon devices are characterized by high efficiency and durability but are mechanically vulnerable, and incompatible with cellulose based substrates. Second generation PV include conventional thin-film technologies, such as amorphous silicon (a-Si), copper-indium-selenide (CIS) or copper-indium-gallium-selenide (CIGS), and cadmium telluride.[121] Compared to first generation PV, these devices have reduced thickness (< 10 μm), which entails a reduction in materials and manufacturing costs, while maintaining excellent stability in many cases but relative lower efficiencies. Second generation solar cells can be fabricated in flexible form and at lower temperatures, and share 4.5% of the global annual PV power production. Finally, new generation PV include emerging thin-film technologies, such as organic photovoltaics (OPV),[122] dye-sensitized solar cells (DSSC),[123] quantum dots photovoltaics (QDPV)[124] and perovskite solar cells (PSC).[125] Emerging solar technologies are still at a research and development scale, or in some cases recently commercialized on a niche production scale. The main advantages of emerging PV are: solution processability and printability; low cost; potential application on flexible and light-weight substrates; semi-transparency; good performance under normal and diffused incident light and even under indoor lighting.[126,127] However, lifetime (and in most cases efficiencies except for perovskite solar cells where values have exceeded 22%[128] of these devices under standard test conditions is still consistently lower compared to conventional PV.

Table 3. Summary of PV devices fabricated on cellulose substrates or including a paper-based component, with at least one layer deposited by printing techniques.

Technology	Substrate	Transparent electrode	Back electrode	Printed layer	Printing technique	PCE	Area	Stability	Ref.
a:Si:H	P_e:smart Type 2 paper	IZO (200 nm) (RF magnetron sputtering)	Al (80nm)/ Ag (40 nm) (evaporation)	Hydrophilic mesoporous coating	Cast-coating	3.40%	0.05 cm^2	Stable after 20 cycles 20 mm radius	[4]
a-Si:H	P_e:smart Type 2 paper	Ag grid (700 nm)	Ag (200nm) /ZnO:Al (80nm) (RF magnetron sputtering)	Hydrophilic mesoporous coating, photoresist	Cast-coating, spin-coating	5.50%	0.5 cm^2	-	[110]
a-Si:H	Printing paper	ITO (RF magnetron sputtering)/Au grid	Au grid (evaporation)	Acrylate lacquer	Doctor-blading	6.70%	0.08 cm^2	-	[99]
CuInSe2	Bacterial nanocellulose paper	ZnO/ITO (RF magnetron sputtering)	Cr (10 nm)/Au (80 nm) (evaporation)	$CuInSe_2$, CdS	Spray-coating, chemical bath deposition	2.25%	0.08-0.15 cm^2	Stable after 120 bending cycles (5 mm radius); 80% of initial PCE maintained after folding- unfolding	[101]
OPV	Amylum coated cellulose	LiF:Al (30 nm, coevaporation)	Au (120 nm, RF magnetron sputtering)	PEDOT:PSS, P3HT:PCBM	Dipping, spin- coating	0.13%	0.13 cm^2	-	[46]
OPV	NFC	ITO (RF magnetron sputtering)	Ag (200 nm) (evaporation)	PEDOT:PSS, P3HT:PCBM	Spin-coating	0.21%	ND	-	[56]
OPV	PE/carton/PE	Al (5 nm)/Ag (15 nm) (evaporated)	PEDOT:PSS (drop-casting)	PEDOT:PSS, P3HT:PCBM	Spin-coating	0.40%	0.18 cm^2	-	[108]
OPV	Glossy paper	PEDOT:PSS (flexographic printing)	Zn (transfer printing)	PEDOT:PSS, Zn, P3HT:PCBM	Flexographic, transfer and gravure printing	1.31% (at 60 mW cm^2)	0.09 cm^2	-	[9]
OPV	CNC	Ag (20 nm) (evaporation)	Ag(100nm) (evaporation)	ZnO:Al, PEI, PFDTBTP:PCBM	Spin-coating	1.40%	0.09 cm^2	-	[59]
OPV	CNC	Ag (20 nm) (evaporation)	Ag (150 nm) (evaporation)	PEIE, PBDTTT-C:PCBM	Spin-coating	2.70% (95 mW cm^2)	ND	-	[61]
OPV	NFC	Ag nanowires (drop-casting)	Al (60 nm) (evaporation)	Ag NW, PEDOT:PSS, P3HT:PCBM	Drop-casting, spin-coating	3.20%	0.09 cm^2	Stable after folding cycles	[63]
OPV	PET	ITO/Ag/ITO (sputtering)	Cellulose/Graphene nanoplatelets (lamination)	ZnO, PEIE, PffBT4T:PCBM, V_2O_x,PEDOT:PSS	Spray-coating	3.36%	0.15-1 cm^2	Stable after 100 bending cycles at 7mm radius; 12% PCE decrease after 100 cycles at 4 mm	[109]

OPV	CNC	PEDOT:PSS (lamination)	Ag (80 nm) (evaporation)	PEI, P3HT:ICBA	Spin-coating	3.80%	0.01-0.06 cm^2	-	[62]
OPV	Printing paper	MoO_3(8nm)/Ag(13nm)/MoO_3(25nm) (evaporation)	pp-Zn (lamination)	PEIE, PTB7:PCBM	Spin-coating	4.10%	0.10 cm^2	-	[35]
OPV	Tunicate CNC- O-(2, 3-dihydroxypropyl)cellulose nanocomposites	ITO (80 nm) (RF magnetron sputtering)	Ag (100 nm) (evaporation)	ZnO, PTB7:PCBM	Spin-coating	4.98%	0.24 cm^2	-	[70]
OPV	Cellophane	ZnO(40 nm)/Ag(12 nm)/ZnO(40 nm) (magnetron sputtering, spin-coating)	Al (evaporation)	ZnO, PTB7-Th:$PC_{71}BM$	Spin-coating	5.94%	0.06 cm^2	92% of initial PCE maintained after 35 folding cycles	[106]
OPV	Glass[a]	ITO	Al (evaporation)	PEDOT:PSS, PCDTBT:PCBM	Spin-coating	5.88% (13 mW cm^2, diffused)	-	-	[51]
DSSC	Box paper	Pt-coated glass/FTO	Ni (chemical bath)	ZnO	Doctor-blading	1.21%	0.16 cm^2	-	[102]
DSSC	Box paper	Pt-coated glass/FTO	Ni (chemical bath)	Meso-TiO2	Doctor-blading	2.90%	0.25 cm^2	-	[111]
DSSC	Glass[b]	FTO	Pt (evaporation)	TiO_2	Drop-casting	3.55%	0.22 cm^2	96% of initial PCE maintained after 1000h accelerated aging test	[103]
DSSC	Glass[c]	FTO	Pt (drop-casting)	TiO_2, nanocelluose hydrogel, Pt	Screen-printing, drop-casting	4.70%	0.40 cm^2	90% of initial PCE maintained after 1000h accelerated aging test	[129]
DSSC	Printing paper	ITO/PEN	Graphene dots/PEDOT:PSS (dipping)	Meso-TiO_2	Doctor-blading	4.91%	0.16 cm^2	Stable after 150 bending cycles	[100]
QDPV	Glass[d]	FTO	FTO	TiO2, Pt, CdS	Screen-printing, casting, dipping	0.52%	0.40 cm^2	-	[130]
QDPV	Printing paper	Gold-palladium (40 nm) (sputtering)[e]	Multilayered graphene (H2B pencil rubbing)	PEDOT:PSS, CdSe QDs:PTCDA:MuLG	Spin-coating, drop-casting	1.80%	5.00 cm^2	-	[104]
PSC	PowerCoat HD cellulose	MoO_3 (17.5 nm)/ Au (11 nm)/ MoO_3 (18.6 nm) (evaporation)	Au (80 nm) (evaporation)	SnO_2, meso-TiO_2, $CH_3NH_3PbI_3$, Spiro-MeOTAD	Spin-coating	2.70%	0.10 cm^2	PCE=0.16% after 72h in air, no encapsulation	[37]
PSC	TEMPO-oxidized cellulose	TiO_x (40 nm)/Ag (10 nm)/TiO_x (40 nm) (sputtering)	Au (80nm) (e-beam evaporation)	ZnO, $CH_3NH_3PbI_3$, Spiro-MeOTAD	Spin-coating	6.37%	0.17 cm^2	PCE=5.43% after 230h in air, no encapsulation	[57]
PSC	Cellulose	Cu(1 nm)/Au(6 nm) (evaporation)	Carbon (screen printing)	Carbon	Screen-printing	9.05%	0.08 cm^2	75% of initial PCE maintained after 1000 bending	[118]

cycles at 6mm curvature radius

[a)] TEMPO-oxidized cellulose was used as transparent high-haze coating

[b)] Cellulose-based materials constitute electron transport layer (TiO_2-laden paper membrane) and electrolyte (NFC based filler)

[c)] Cellulose-based materials constitute electrolyte membrane (nanocellulose areogel film)

[d)] Cellulose-based materials constitute filler membrane (NFC, TEMPO-oxidized-NFC)

[e)] Both top and back electrode are opaque

4.2.1. Paper-based conventional thin film photovoltaics

Hydrogenated amorphous Silicon

Hydrogenated amorphous silicon (a-Si:H) solar cells are based on a thin (<1 μm) intrinsic a-Si film, sandwiched between two heavily doped a-Si regions; the reduced thickness compared to conventional crystalline Silicon, in addition to potential flexibility, make a-Si:H PV a viable alternative for application where light weight and mechanical compliance are required. The first a-Si:H solar cell on a paper substrate was reported by Águas et al.[4] By implementing a printed hydrophilic mesoporous coating to reduce the paper roughness, flexible a-Si:H solar cells with architecture paper/HM/Al (80 nm)/Ag (40 nm)/n-i-p a-Si:H (355 nm)/IZO (200 nm) delivered a power conversion efficiency (PCE) of 3.40% and fill factor (FF) of 40.7%, open-circuit voltage (V_{OC}) of 0.82 V, short- circuit current density (J_{SC}) of 10.19 mA cm^{-2}, under 0.1 W cm^{-2} AM1.5 conditions. Cells remained fully functional after manual bending at 20 mm radius, due to the flexibility and good adhesion of the different layers of the cell stack on paper.

A substantial improvement in paper-based a-Si:H solar cell performance was reported in the work by Van der Werf et al.[99] The Ag (300 nm)/ZnO:Al (100 nm)/n-i-p a-Si:H (406 nm)/ITO (80 nm)/Au-grid stack was fabricated both on nanoimprinted lacquer-coated paper and stainless steel. The blade-coated nanoimprinted lacquer coating played the dual role of creating a smooth substrate, while reducing at the same time the undesired reflection of the incident light. Interestingly, paper-based solar cells were slightly more efficient than nanoimprinted stainless steel-based devices, mainly due to an increase in V_{OC} (V_{OC} = 897 mV and PCE = 6.7% for paper devices, versus V_{OC} = 811 mV and PCE = 6.5% for stainless steel-based solar cells). This improvement was associated to the lower surface roughness of the lacquer-coated cellulose substrate and to the better texture obtained by nanoimprinting.

Copper Indium Selenide

In addition to amorphous silicon devices, another conventional thin film technology has been recently implemented on cellulose substrates, based on spray-deposited $CuInSe_2$ nanocrystals.[101] The bottom contact was a thermally evaporated Cr/Au bilayer on bacterial nanocellulose paper, covered by spray-coating a $CuInSe_2$ nanocrystals ink as the active layer; afterwards, a CdS buffer layer was deposited by chemical bath deposition, and a ZnO/ITO contact thermally evaporated to complete the stack. Flexible cellulose-based devices delivered a PCE as high as 2.25% and a remarkable stability: the efficiency remained unvaried after 120 mechanical flexing cycles at 5 mm bending radius, and the device maintained more than 80% of its initial PCE after folding and unfolding, as depicted in **Figure** 6.a. The excellent mechanical stability of $CuInSe_2$ paper-based devices is attributed to a stabilization of the top ITO layer determined by the strong adhesion between the active layer nanocrystals and the nanocellulose, that limits the propagation of bending-induced cracks to the top electrode; devices were completely functional after bending at a radius as small as 3 mm.

4.2.2. Paper-based emerging thin film photovoltaics

Organic solar cells

Organic photovoltaic has been the first technology to be transferred from rigid and plastic substrates to cellulose-based substrates. Organic solar cells employ an organic semiconductor (polymer or small molecule), usually sandwiched or blended with a fullerene derivative, to absorb the incident light; after exciton separation, charges are transported and collected at electron and hole selective contacts.[122,131] Being solution-processable and printable, OPV represent a cost-effective alternative to conventional thin film technologies.[132] Even though, in 2005 Lamprecht et al. demonstrated an organic photodiode on a newspaper,[42] it was only in

2010 when the first organic solar cell was developed on paper.[46] The device structure consisting in an Au/PEDOT:PSS/P3HT:PCBM/LiF:Al stack fabricated on amylum-coated cellulose delivered a PCE of 0.13% under standard testing conditions (STC, 1 Sun, AM 1.5G, 25°C).

Small improvements were made by employing highly transparent nanopaper prepared from nanofibrillated cellulose (NFC) as a substrate for OPV.[56] The high haze offered by nanopaper was beneficial in terms of light absorption in the active layer. However, solar cells with a device stack composed of NFC/ITO/PEDOT:PSS/P3HT:PCBM/Ca/Al, with the HTL and active layers deposited by spin-coating, only delivered a PCE of 0.21% at STC; the poor efficiency was mainly affected by the low FF determined by the high sheet resistance of the NFC/ITO electrode. The PCE was greatly enhanced by replacing ITO with transparent conductive films of Ag nanowires (NWs).[63] An Ag NWs water suspension and a NFC dispersion were sequentially cast and dried on a silicon wafer; after complete drying, Ag NWs-coated nanofibre paper was obtained.. By printing PEDOT:PSS and P3HT:PCBM layers and evaporating the metallic cathode, a flexible and foldable paper-based solar cell with 3.20% PCE at STC was fabricated; the device was capable of generating power also during and after folding. J-V characteristics and photographs of device are shown in Figure 6.b.

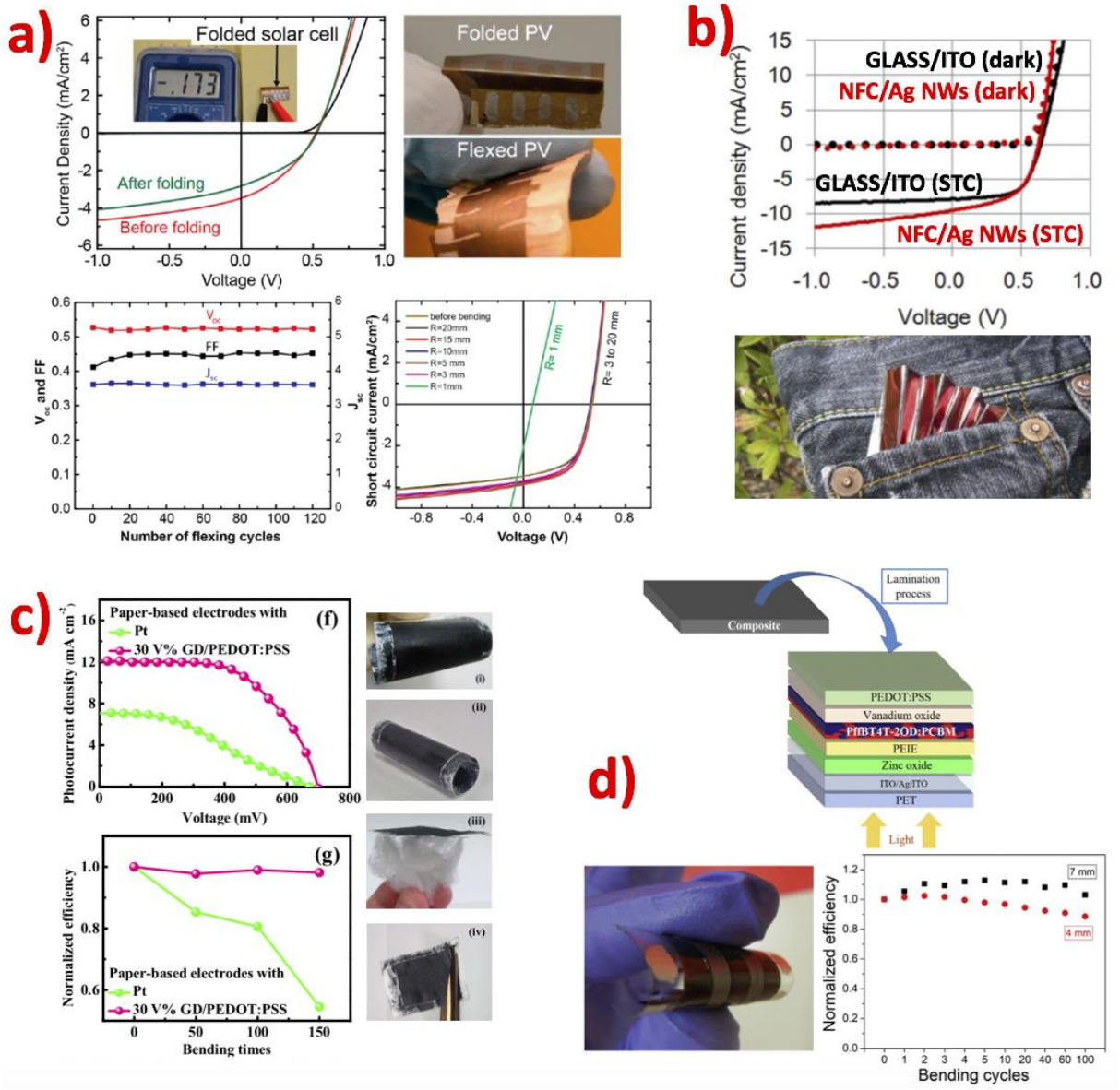

Figure 6. a) Flexible and foldable Cr/Au/$CuInSe_2$/CdS/ZnO/ITO solar cell on bacterial cellulose: top left, J-V curves of the device measured in a pristine state (red curve) and after folding (red curve), with inset picture showing that the solar cell maintains its functionality even when folded; top right, photographs of the folded and bended $CuInSe_2$ paper solar cell; bottom left, average photovoltaic parameters (statistics over four samples) of $CuInSe_2$ devices as a function of the number of flexing cycles at 5 mm bending radius; bottom right, J-V curves of a CuInSe2 solar cell before bending and after bending at radii from 20 to 1 mm**.** Reproduced with permission. [101] Copyright 2017, American Chemical Society. b) Foldable organic solar cells on AgNWs-coated nanofibrillated cellulose (NFC): on the top, J-V curves in the dark (dotted lines) and at STC (continuous lines) of glass/ITO/PEDOT:PSS/P3HT:PCBM/Al (black lines) and NFC/Ag NWs/PEDOT:PSS/P3HT:PCBM/Al (red lines) solar cells; on the bottom, picture of the foldable organic solar cell**.** Reproduced with permission. [63] Copyright 2015, Nature. c) Top left, J-V curves of flexible DSSCs fabricated with PEN/ITO/N719-sensitized TiO_2

photoanodes and paper counter electrodes based on printed graphene dots (GD)/PEDOT:PSS (pink curve) or sputtered Pt (green curve); bottom left, normalized efficiency versus bending cycle of the same devices; on the right, photographs of paper based GD/PEDOT:PSS counter electrodes, highlighting their flexibility and light weight. Reproduced with permission. [100] Copyright 2017, Elsevier Ltd. d) On the top, structure of a flexible fully sprayed ZnO/PEIE/PffBT4T-2OD:$PC_{70}BM$/V2Ox/PEDOT:PSS organic solar cell fabricated on PET/ITO/Ag/ITO bottom electrode and assembled with a laminated cellulose-graphene top electrode; bottom left, photograph of the flexible organic solar cell; bottom right, normalized device efficiency versus bending cycles at bending radii of 7 nm (black data points) or 4 mm (red data points). Reproduced with permission. [109] Copyright 2018, Elsevier Ltd. All rights reserved.

An alternative to NFC nanopaper is represented by cellulose nanocrystals nanopaper (CNC). CNC films are composed of rigid rod-like crystalline nanoparticles and characterized by a lower roughness than NFC,[133] therefore being an excellent candidate as a substrate for printed OPV. A comparison between CNC and NFC substrates was carried out by Vilhegas Costa et al. [59] Devices with architecture Ag (100 nm)/ZnO:Al/PEI (10 nm)/PFDTBTP:PCBM (300 nm)/MoO_3 (8 nm)/Ag (20 nm), with spin-coated electron transport and active layers, were fabricated on CNC and NFC substrates. Interestingly, a PCE of 1.40% was obtained for the former, while the latter delivered 0.50% PCE; the poor performance of NCF devices was due to the fibrous, heterogeneous and rough surface of the NFC film, that in turn resulted in higher device series resistance compared to CNC-based solar cells. Zhou et al. [61] developed an organic solar device with architecture Ag (20 nm)/PEIE (10 nm)/PBDTTT-C:PCBM (90 nm)/MoO_3 (15 nm)/Ag (150 nm) on CNC substrate. Due to the extremely low surface roughness of the substrate (RMS 1.8 ± 0.6 nm), no planarizing layer was required for device fabrication. The transmittance losses observed in the film were attributed to scattering effects, which are beneficial for light absorption in the active layer. The substrates also showed better wettability compared to bare glass; the semi-transparent 20 nm thick Ag electrodes evaporated on top of CNC substrates showed long-range conductivity, being above the percolation

threshold, while their glass-based counterparts were found to be not conductive. Printing of the electron collecting and active layers did not damage the CNC substrate, that is compatible with organic solvents; consequently, an average PCE of 2.70% was demonstrated for inverted CNC-based OPV devices.

The efficiency of CNC-based OPV was further boosted in a subsequent work from the same group.[62] The performance enhancement was determined by replacement of the Ag semi-transparent bottom electrode with a transparent conductive PEDOT:PSS layer, produced by film-transfer lamination, as top contact; the resulting architecture was CNC/Ag (80 nm)/PEI (10 nm)/P3HT:ICBA (200 nm)/PEDOT:PSS (100 nm). The lamination technique was adopted in order to overcome the incompatibility of water-based PEDOT:PSS with the CNC substrate. A remarkable average PCE of 3.80% was achieved with this architecture; nevertheless, the solar cell yield (ratio between working and shunted devices) was compromised by the large height variation in the CNC film, dependent on the substrate fabrication process.

Among paper substrates for OPV, a commonly used, cheap alternative is represented by the carton generally used for beverage storage; fabrication of solar cells on this challenging substrate is not trivial.[108] Carton for packages is composed by a pulp layer sandwiched between polyethylene films; due to its poor wettability, unchanged even after surface treatments, drop-casting was chosen for the deposition of conductive PEDOT:PSS; the solar cell structure was completed with a spin-coated P3HT:PCBM active layer and an evaporated semi-transparent Al (5 nm)/Ag (15 nm) cathode. Even though representing a cost-effective approach towards roll-to-roll, solution-processable paper-based OPV, the PCE of the device was limited to 0.40%, because of the low optical transparency of the top electrode.

An important step towards roll-to-roll solar cell fabrication was represented by the development of a fully-printed Zn/ZnO/P3HT:PCBM/PEDOT:PSS device fabricated on glossy paper.[9] The Zn film was transfer-printed on the cellulose substrate; ZnO was obtained from oxidation of the

metallic film. Subsequently, the active layer was deposited by gravure printing, by using a standard doctor-blade; finally the transparent top electrode was deposited by flexographic printing of a PEDOT:PSS ink. A PCE of 1.31% was achieved for the fully-printed device; the J-V curve, characterized by a marked S-shaped was attributed to the low quality of the ZnO-PCBM interface.

To improve the performance of paper solar cells, in addition to optimizing substrates, electrodes and fabrication processes, the device active layer must be carefully optimized by choosing highly efficient materials. Very high efficiencies have been obtained by fabricating cellulose-based devices with a PTB7:PCBM bulk heterojunction active layer. Leonat et al.[35] employed the low band gap PTB7 polymer to fabricate inverted OPV with a metal-dielectric-metal top contact. The bottom contact was deposited with a roll-to-roll compatible process by laminating a polypropylene/Zn foil on common printing paper; the native thin ZnO layer naturally formed on top of the metallic foil. PEIE and the PTB7:PCBM active layer were then spin-coated, and a MoO_3 (8 nm)/Ag (13 nm)/MoO_3 (25 nm) thermally evaporated, with the last oxide layer acting as an anti-reflection coating. The cellulose OPV device delivered a PCE of 4.1% (J_{SC} 10.6 mA cm^{-2}, V_{OC} 710 mV, FF 55.0%).

PTB7:PCBM blends have also been employed by Cheng et al. to fabricate paper-OPV with a remarkable PCE of 4.98%.[70] In this work, a nanocomposite paper was developed by introducing a rigid percolating network of tunicate cellulose nanocrystals (TCNC) in a soft 0-(2,3-dihydroxypropyl)cellulose (DHPC) matrix; the filler improves the mechanical properties of DHPC, without compromising its transparency. The excellent adhesive properties of the nanocomposite paper enabled the fabrication of a flexible ITO (80 nm)/ ZnO (30nm)/ PTB7:PCBM (100 nm)/MoO_3 (10 nm)/ Ag (100 nm) device, delivering a PCE of 4.98% (J_{SC} 13.7 mA cm^{-2}, V_{OC} 710 mV, FF 51.4%), among the highest reported so far for organic solar cells on cellulose.

Record PCE has been achieved by using a spin-coated PTB7-Th:$PC_{71}BM$ blend as the active layer for paper-based OPV. Li et al. [106]developed a foldable organic solar cell on an ultra-thin cellophane substrate; conductivity of the transparent cellophane film was obtained by deposition of a ZnO/Ag/ZnO electrodes by magnetron sputtering and subsequent spin-coating of the metal oxide extracting layer; the stack was completed by thermally evaporating a MoO3 interlayer and an Al back electrode. Devices exhibited a PCE as high as 5.94% and a power weight ratio of 2.11 W g^{-1}. Foldability and excellent mechanical properties were demonstrated as the device preserved 92% of its initial PCE after 35 folding cycles and 98% of the efficiency after 500 bending cycles at a curvature radius of 1 mm.

La Notte et al.[109] reported a flexible fully sprayed organic solar cell with a graphene nanoplatelets (GnPs)/cellulose composite as opaque top electrode. The ZnO/PEIE/PffBT4T-2OD:$PC_{70}BM$/V_2O_x/PEDOT:PSS device stack was fabricated on top of PET/ITO/Ag/ITO bottom electrodes and the structure completed by laminating a spray-coated GnPs/cellulose top electrode, as shown in Figure 3.d. Small area devices delivered a PCE of 2.85% and a remarkable mechanical resistance to bending; moreover, compatibility of the laminated cellulose composite electrodes with large area devices was demonstrated, showing the high potential of GnPs/cellulose composite layers for scaling-up of paper based organic solar cells, particularly when even the plastic substrate can be replaced with a cellulosic alternative.

Dye-sensitized solar cells

Dye-sensitized solar cells (DSSC) are a PV technology inspired by the principle of the photosynthesis: a photosensitive dye at the anode of the device is responsible for light harvesting; when the dye absorbs the incident light, it transitions to an excited state; charge is injected into an electron transport layer with favorable energy levels, usually a semiconducting oxide; the oxidized dye is then regenerated by an electrolyte, sandwiched between the sensitized photoanode and the counter electrode. This structure has been optimized on glass and

plastic.[134,135] There have been growing attempts at making the fabrication more sustainable.[136] Recently DSSCs have been fabricated on cellulose substrates. For example, Ni-coated box paper has been used as opaque electrode for DSSCs with a N719-sensitized ZnO photoanode and a glass /FTO/Pt counter electrode, reaching a PCE of 1.21% (V_{OC} 560 mV, J_{SC} 6.70 mA cm^{-2} and FF 33%) at STC. Noteworthy, Ni-coated electrodes were fully covered by ZnO and resistant to the electrolyte corrosion.[102] To enhance the performance, ZnO was replaced with a binder-free TiO_2 blade-coated layer; in fact, at the low process temperature characterizing paper substrates, the removal of organic binders usually employed for TiO_2 paste formulation is hindered,[137] and electron transport in the semiconducting layer can be negatively affected. Good film forming properties were observed for TiO_2-coated Ni-paper and no cracks appeared in the layer after bending the electrode;[137] N719-sensitized electrodes were assembled with a glass/FTO/Pt counter electrode and filled with a iodine-free electrolyte to deliver 2.90% conversion efficiency (V_{OC} 650 mV, J_{SC} 7.97 mA cm^{-2} and FF 56%).[111] Even though the electrodes were characterized as being highly bendable, device flexibility was lost when completing the stack with a rigid glass-based counter electrode. Full flexibility was indeed preserved for paper-DSSCs fabricated with graphene dots (GD)/PEDOT:PSS/printing paper counter electrodes.[100] The counter electrode was used in combination with a sensitized doctor-bladed binder-free TiO_2 layer on flexible PEN/ITO. The porosity of the paper was greatly reduced by infiltration of the GD/PEDOT:PSS composite, leading to a high PCE of 4.91%, that was stable even after 150 bending cycles. The photovoltaic characteristics of flexible DSSCs with a GD/PEDOT:PSS paper counter electrode or a sputtered Pt reference counter electrode, together with their normalized efficiency versus bending cycles and photographs of the light-weight, flexible, space saving GD/PEDOT:PSS counter electrodes, are shown in Figure 3.c.

In addition to bendable substrates, cellulose-based materials have been employed also as membranes for DSSCs components. For example, Bella et al. reported the development of a

TiO_2-laden cellulose photoanode, applicable in principle to different substrates, such as glass or plastic. The sensitized paper-based photoanode was used in combination with a NFC-filled polymer electrolyte membrane to obtain a quasi-solid state paper-DSSC; the remarkable 3.55% PCE obtained at STC remained stable (96% of the initial PCE) after 1000 h of accelerated aging test.[103] Several advantages are associated with the use of an electrolyte-filled cellulose membrane, such as a more homogeneous electrolyte distribution compared to the vacuum-filling technique, and the possibility to prepare the electrolyte by simple printing techniques. A highly porous nanocellulose aerogel was developed by means of screen-printing as membrane for organic liquid electrolytes in DSSC.[129] Replacement of conventional liquid electrolytes with an impregnated nanocellulose membrane enabled a simplification of the fabrication process, without compromising the charge transfer resistance at the counter electrode, the diffusion of the electrolyte and the stability of the device.

Quantum dots solar cells

Quantum dots photovoltaics (QDPV) are based on zero-dimensional semiconductors. Nanostructured semiconductors with three dimensions in the nanometer scales are characterized by exceptional optical and electronical features that can be tuned by changing the dots size, due to quantum confinements effects. Tunability of the band gap, in addition to the solution-processability and printability of these materials, make QDs highly desirable as light absorbers in solar cells. QDPV devices have been demonstrated on paper substrates by Dasari et al.[104] A novel "calligraphic solar cell" was designed and fabricated on common printing paper by developing a multilayered graphene electrode; the conductive electrode was obtained by simply rubbing a H2B pencil on paper. After spin-coating a thin PEDOT:PSS HTL, a CdSe-QDs:multilayered-graphene:PTCDA active layer was deposited by drop-casting, and Au-Pd thermally evaporated as top electrode. MulG played a dual role in the device, that is electrode material and charge transporter at the active layer interface. A PCE of 1.80% (I_{SC} 2.3 mA cm^{-}

^{2}, 775 mV) was delivered by this low-cost, easy-to-fabricate solar cell based on common printing paper.

Cellulose materials were used as electrolyte-filled membranes also in quantum dot sensitized solar cells (QDSSC).[130] Membranes were developed by using bacterial cellulose, NFC, chitin nanofibres and TEMPO-oxidized NFC, and the effect of different surface functional groups and fibrillar structures was investigated; cellulose was demonstrated as a good candidate for electrolyte carrier membranes, as devices with architecture glass/FTO/TiO_2/CdS-QDs/aerogel:electrolyte/Pt/FTO/glass exhibited a modest PCE between 0.46 and 0.52%, comparable to the liquid electrolyte based reference, for all the cellulose aerogels under investigation.

Perovskite solar cells

Perovskite solar cells (PSC) are the latest trend in the photovoltaic field. Initially developed from DSSCs, PSCs have experienced an increasing interest from the scientific community and a meteoritic rise in performances in the last decade. The active layer is composed of a hybrid organic-inorganic crystalline material with perovskite structure, usually a mixed metal-organic halide compound. PSC have been fabricated both in n-i-p and p-i-n configurations on a wide variety of different flexible substrates. [79] Deposition of the perovskite layer can be carried out at low temperatures, thus being compatible with cellulose-based materials. However, the application of PSCs to paper-based substrates is still at its pioneering stages. Castro Hermosa et al. fabricated a flexible mesostructured n-i-p perovskite solar cell on Au-coated opaque paper shown in Figure 4a; the top transparent electrode, optimized in order to achieve a compromise between transparency and conductivity, was fabricated by thermal evaporation in a dielectric-metal-dielectric (MoO_3/Au/MoO_3, MAM) configuration.[37] The remaining layers were fabricated by spin-coating. Growth of the perovskite layer was enabled by the development of a low-T, UV-cured mesoporous TiO_2 scaffold. Solar cells with paper/Au (80 nm)/SnO_2/meso-

$TiO_2/CH_3NH_3PbI_3$/spiro-MeOTAD/MoO_3 (17.5 nm)/Au (11 nm)/MoO_3 (18.6 nm) architectures were tested under STC and an efficiency of 2.70% was obtained (J_{SC} 8.9 mA cm^{-2}, V_{OC} 610 mV, FF 51%), that is among the highest reported for a printed solar cell directly deposited on an opaque paper substrate. The stack was tested also on PET rather than on paper; illumination from the ITO side determined a dramatic increase in the solar cell photocurrent, from 9.1 to 14.9 mA/cm^2, compared to the MAM side illumination case, suggesting that further optimization of the MAM electrode transparency could lead to a favourable enhancement of the performance of paper-PSCs.

Jung et al. fabricated a color tunable flexible perovskite solar cell by using a transparent TEMPO-oxidized nanocellulose paper; this substrate is characterized by high transmittance and haze, of 90% and 80% respectively, therefore being particularly suited for application in solar cells. After treating the cellulose substrate with a hydrophobic material, the transparent TiOx/Au/TiOx bottom electrode was deposited by sputtering; the ZnO/perovskite/spiro-MeOTAD stack was subsequently deposited by spin-coating and the top Au electrode fabricated by e-beam evaporation. Paper-based devices delivered a maximum PCE of 6.37% (J_{SC} 15.4 mA cm^{-2}, V_{OC} 860 mV, FF 48%), that decreased to 5.43% after storing the device for 230 h in air.[57]

The highest PCE achieved to date among all cellulose-based solar devices has been recently reported by Gao et al. [118]. Highly efficient perovskite solar cells were fabricated on screen-printed carbon-paper back electrodes by using an inverted device architecture, that is paper/C/$CH_3NH_3PbI_3$/C_{60}/BCP/Cu/Au. All layers apart from the electrodes were fabricated by vacuum deposition and the ultrathin Cu/Au metallic film thermally evaporated. Successful back electrode optimization in terms of hydrophobicity, roughness, sheet resistance and perovskite wettability, enabled the fabrication of a 9.05% efficient hole-transport material-free perovskite solar cell with excellent mechanical properties. Devices maintained 75% of their initial PCE

after 1000 bending cycles at 6 mm curvature radius, thus showing the feasibility of cellulose-based perovskite devices for flexible and wearable applications.

4.3. Performance enhancement

Solar cell performance can be enhanced by light management, by increasing the absorbed light through introduction of antireflective paper-based coatings or by using efficient light-scattering cellulose substrates. Porous cellulose has the capability of inducing a broadband, angle insensitive light scattering at the air/solar cell interface, which has the beneficial effect on the absorbed light, and therefore on device photocurrent and efficiency. Ha et al.[51] employed a low-cost and easy to process transparent cellulose film to enhance the performance of GaAs solar cells. When adding TEMPO-oxidized transparent cellulose on top of a GaAs device, the reflectivity was reduced from 35-45% to 15-25%; because of the highly-textured cellulose surface, the angle-dependent reflectivity was also decreased. This effect translated to a higher external quantum efficiency of the device, and 20 % and 24% enhancement of the J_{SC} and PCE respectively. Light scattering can be enhanced also through R2R compatible and low-cost UV-nanoimprint of OrmoComp® (Figure 5c); for example a PCE of 5.5% was obtained on textured printing paper with a Ag (200 nm)/ZnO:Al (80 nm)/n-i-p a-Si:H (335 nm)/ZnO:Al (80 nm)/Ag (grid, 700 nm) device architecture [110] Surface modification combined with reflectance of Ag (200 nm)/AZO (80 nm) electrode increased the light trapping on solar cell.

Enhanced performance under diffuse light conditions was observed also for glass/ITO/PEDOT:PSS/PCDTBT:PCBM/Ca/Al organic solar cells with a TEMPO-oxidized cellulose coating attached on the glass substrates; by illuminating the cellulose-coated device with 13 mW cm^{-2} diffused light, the PCE was increased from 5.34 to 5.88%. The authors attribute this effect to the ultra-high transmittance and ultra-high haze paper coating.[51]

4.4. Issues and further studies

There are several drawbacks when a metal is directly deposited on a rough paper such as inhomogeneous film growth or low adhesion. Lamprecht et al. [42] reported the first photodiode fabricate on paper and before the evaporation of bottom gold electrode (55nm), the highly rough surface of paper substrate (>50 um) was planarized with an organic-inorganic hybrid polymer (ORMOCER®).[138] ORMOCER layer was spin coated in an inert Ar atmosphere at 4000 rpm for 45 s and annealed at 120 °C for 90 min. The resulting thick layer (100 µm) reduced the average paper roughness to less than 3 nm. Similar planarization process was reported by Van der Werf et al.[99] who blade coated an UV-curable acrylate lacquer on top of paper followed for the deposition of Ag(300 nm)/AZO(100 nm) electrode. Also, the cast-coating of a hydrophilic mesoporous layer (HM) on top of the highly porous printing paper created a smooth surface (RMS roughness of 9.42 nm) with excellent wettability and nanoscale porosity. The substrate was fully compatible with device fabrication, being thermally stable up to 250°C and showing after the heating process improved surface properties and minimum gas desorption, that could lead to contamination of the active layer.[4] Planarization process avoid the device short-circuit between the electrodes, [42,62] prevents the cell cracking[4] and retains constant the electrical field of solar cell[105] which can vary with the surface roughness; however, the planarization polymer must be carefully selected because a wrong choice (i.e Polyethylene) can increase the hydrophobicity of paper substrate.[108]

5. Energy storage on paper.

In this section an overview on paper-based supercapacitors and batteries, whose performances are reported in Table 4, is presented focusing on the technological issues and the achieved results obtained on every technology.

5.1. Supercapacitors on paper

Electrochemical supercapacitors (ES), may be an alternative to batteries in electrical energy storage applications when high power delivery or absorption is required. In fact, the ES are power devices that can be completely charged or discharged in a few seconds; as a result, their energy density is lower than that of batteries. In general, supercapacitors, in terms of storable energy density, fill the gap between conventional solid-state batteries and electrolytic capacitors. The combination of pseudo-capacitive nanomaterials, with nanostructured lithium electrodes or the use of carbon nanotubes, has brought the energy density of the hybrid supercapacitors closer to that of the batteries. An electrochemical supercapacitor consists of two electrodes, an electrolyte and a separator that electrically isolates the two electrodes. Depending on the materials used to make the electrodes, the charge storage mechanism changes, so it is possible to distinguish different types of ES.[139,140]

In **Figure** 7, the different types of supercapacitors are reported, divided according to their architecture (sandwiched between two sheet of paper, planar architecture prepared on paper substrate and double faced architectures where paper acts as support and as separator), type of electrodes (symmetric or asymmetric), material used for the electrodes (carbon based which are used for electrostatic non faradic supercapacitor, metal oxides and polymers which are used to realize pseudo-capacitors, faradic capacitors, and hybrid electrodes), type of supercapacitors (electrostatic, non faradic, pseudocapacitor or faradic, hybrid).

Table 4. Summary of paper-based storage devices characteristics and performance.

Storage system	Substrate	Electrode	Electrolyte	Printed layers	Printing technique	Device assembly	Capacity/ capacitance	CSC [$F \cdot g^{-1}$]	Energy density	Power density	Ref
I-S	Paper-kimwipess	SWCNT/PANI	H_3PO_4/PVA	Electrodes	Impregnation	Lamination	330 mF cm^{-2}	533	--	--	[141]
E-S	Paper-kimwipess	SWCNT	H_3PO_4/PVA	Electrodes	Impregnation	Lamination	46 mF cm^{-2}		--	--	[141]
F-S	Paper-kimwipess	PANI	H_3PO_4/PVA	Electrodes	Impregnation	Lamination	106 mF cm^{-2}	160	--	--	[141]
F-S	Common printing paper	PPy	H_3PO_4/PVA	Electrodes	Impregnation	Lamination	420 mF cm^{-2}	--	1 $mWh \cdot cm^{-3}$	0.27 $W \cdot cm^{-3}$	[87]
F-S	Commercial paper Korean Hanji (mulberry)	MnO	N_2SO_4/PVA	Electrodes	Ligand mediated assembly	Lamination (gel electrolyte and liquid electrolyte)	617 mF cm^{-2}	481	--	--	[43]
I-S	Commercial paper Korean Hanji (mulberry)	MnO/Au	N_2SO_4/PVA	Electrodes	Ligand mediated assembly	Lamination (gel electrolyte and liquid electrolyte)	1350 mF cm^{-2}	709	--	--	[43]
I-S	Carbon fibre paper	PEDOT/ CNT	$BMIBF_4$	Electrodes/ Elctrolyte	Polymerization/drop casting	Lamination (gel electrolyte and liquid electrolyte)	85 mF cm^{-2}	154	6.5 $Wh \cdot Kg^{-1}$	11.3 $KW \cdot Kg^{-1}$	[142]
E-S	Filter paper	Graphene	H_2SO_4/PVA	Electrodes/electrolyte	Vacuum Filtration	Soaking of the two electrodes in the gel electrolyte then press	46 mF cm^{-2}	--	6 $\mu Wh \cdot cm^{-2}$	1 $mW \cdot cm^{-2}$	[54]
E-S	Paper	CNF	KOH	--	--	--	2.45 mF cm^{-2}	11	0.035 $Wh \cdot Kg^{-1}$	3150 $W \cdot Kg^{-1}$	[143]
E-S	Paper	CNF/DWCNT	KOH	--	--	--	27.16 $mFcm^{-2}$	163	3.6 $Wh \cdot Kg^{-1}$	24.8 $W \cdot Kg^{-1}$	[143]
E-S	Paper	CNF/MWCNT	KOH	--	--	--	14.34 mF cm^{-2}	241	4.1 $Wh \cdot Kg^{-1}$	19.6 $W \cdot Kg^{-1}$	[143]

I-S	Paper	PEDOT/CNT/Ag	H_3PO_4/PVA	Electrodes/electrolyte	Inkjet/drop casting	Mutifinger on which the electrolyte was drop casted	26.6 mF cm^{-3}	--	42.1 mWh·cm^{-3}	89.1 mW·cm^{-3}	[144]
S	Whatman *filter paper*	PPy/NF	Na_2SO_4	Electrodes	Impregnation	Electrodes with porous polyethylene membrane in liquid electrolyte then press	3,32 mF cm^{-2}	--	--	--	[145]
S	Whatman *filter paper*	PPy/CNT	Na_2SO_4	Electrodes	Impregnation	Electrodes with porous polyethylene membrane in liquid electrolyte then press	2,42 mF cm^{-2}	--	--	--	[145]
S	Whatman *filter paper*	MnO2/NP	Na_2SO_4	Electrodes	Impregnation	Electrodes with porous polyethylene membrane in liquid electrolyte then pressed	2,14 $mFcm^{-2}$	--	--	--	[145]
I-S	Bacterial cellulose	PPy/CuO	NaCl	Electrodes	Immersion	-	--	601 $F{\cdot}g^{-1}$	48.2 Wh·kg^{-1}	85.8 W·kg^{-1}	[146]
E-B	Glossy paper, copy paper	Zinc-Carbon-PEDOT/Air	LiCl/LiOH	Electrodes/reservoir for electrolyte	Screen printing, Inkjet printing	-	0.5mAh cm^2	--	--	--	[147]
E-B	Filter paper	Cellulose-PPy conductive paper composite	NaCl	--	Polymerization/infiltration	-	50 mAh cm^2	--	--	--	[148]
E-B	Paper	Cu - Al	H_2O	Electrodes	Evaporation	-	--	--	--	70 nW cm^{-2} – 350 $\mu W/cm^2$	[149–151]
E-B	Filter Paper	Ag-Al	H_2O	Electrodes	Screen printing	Origami 3D assembly	--	--	--	0.52 $mJcm^{-2}$	[152]
E-B	Tatoo paper	Ag-Zn	H_2O	Electrodes	Screen printing	Sealing of the parts	1.48 $mAhcm^{-2}$	--	--	--	[153]

						using epoxy glue					
LIB	Xerox paper	$LiMn_2O_4$-CNT and $Li_4Ti_2O_{12}$-CNT	$LiPF_6$	Electrodes	Meyer rod coating	Pouch-type cell assembly	110 mAh g^{-1}	--	--	--	[48]
LIB	Xerox paper	$Li_4Ti_2O_{12}$-CNT	$LiPF_6$	Electrodes	Meyer rod coating	Lamination	147 mAh g^{-1}	--	108 mWh g^{-1}	--	[154]
LIB	Paper fabricated from pulp	Si-CNT	$LiPF_6$	Electrodes	Meyer rod coating	Pouch-type cell assembly	2000 mAh g^{-1}	--	--	--	[155]
Li-O_2	Paper	Carbon nanoparticles (size 50 nm)	$LiCF_3SO_3$ in Tetraethylene glycol dimethyl ether (TEGDME)	Electrodes	Brush painting	Pouch-type cell assembly	1000 mAh g^{-1}	--	--	--	[156]

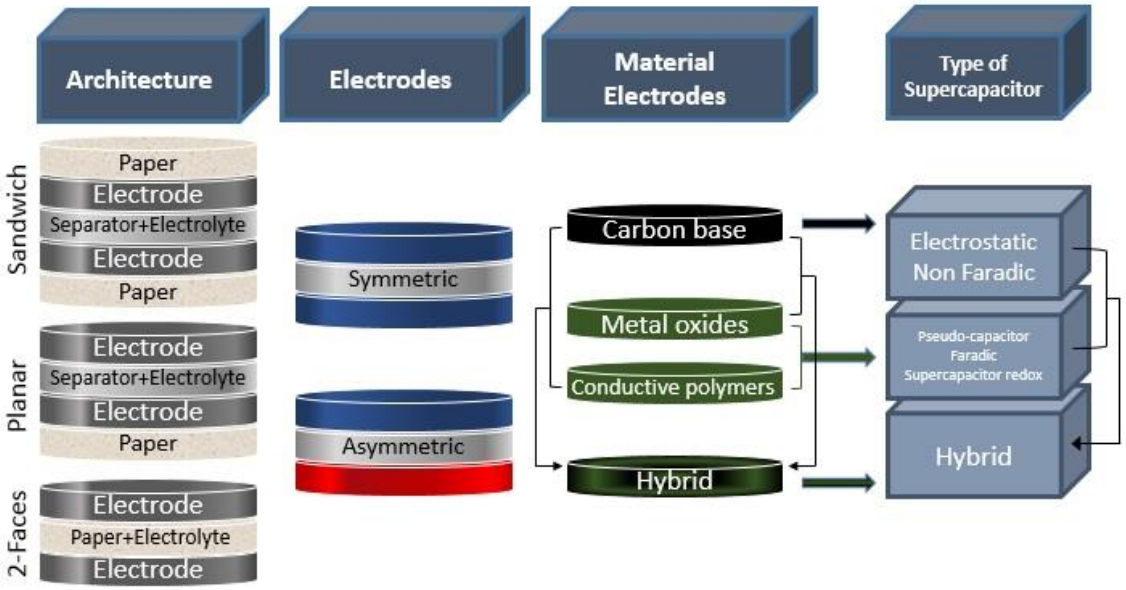

Figure 7. Classification of supercapacitors according to type of architecture (sandwich, planar, double faced), electrodes (symmetric or asymmetric), materials used for electrodes and type of supercapacitor.

The electrostatic supercapacitors (electrostatic double-layer capacitors, EDLS), are currently the most common devices, and use carbon-based materials absorbed on paper to prepare electrodes with a high surface area and high porosity.[157] Such materials are not electrochemically active and, therefore, there is no electrochemical reaction on the electrode material during the charging and discharging processes of the ES, consequently there is no accumulation of pure physical charge at the electrode / electrolyte interface. These types of supercapacitors store energy on the two electrode / electrolyte interfaces using surface dissociation and ion adsorption. The electric charges in excess are accumulated on the electrode surfaces and the electrolyte ions are accumulated on the electrolyte side to balance the charge at the electrode / electrolyte interface. During the charging process, the electrons travel from the negative electrode to the positive electrode through an external circuit, while inside the

electrolyte, the cations move towards the negative electrode and the anions move towards the positive electrode. During the discharge, the inverse process takes place. This surface storage mechanism allows energy to be released and absorbed in a very short time. However, these devices suffer from a limited specific capacity and a limited energy density. [139,140]

Other types of supercapacitors are faradic supercapacitors (FS), also known as pseudo-condensers or redox supercapacitors, in which the material used for the electrode is electrochemically active. On these electrodes, rapid and reversible faradic reactions that involve the passage of the charge through the double layer, occur.This process is similar to the charge and discharge that occurs in the batteries, with the consequent passage of current through the cell of the supercapacitor. In this type of supercapacitor, the charges can be stored directly during the charging and discharging processes. The materials used in the electrodes of these types of supercapacitors are metal oxides such as ruthenium oxide (RuO_2), cobalt oxide (Co_3O_4), ferric oxide (F_3O_4) or manganese oxide (MnO_2) or polymers with high conductivity and high specific capacity such as polypyrrole (PPy), polyaniline (PANI) and polythiophene (PEDOT). [158] FSs have much greater energy capacity and density values than an EDLS, since electrochemical processes occur on a certain volume of the electrode near the electrolyte interface, and not just on the surface. Nevertheless, an FS exhibits lower stability and power density than an EDLS, because faradic processes are normally slower than non-faradic processes. [139,140]

Electrostatic and faradic supercapacitors can also be classified as symmetric supercapacitors if they use the same type of electrodes or as asymmetrical if there are two differente electrodes. The latest generation of supercapacitors is developed using an asymmetrical electrode configuration. These usually include an electrode consisting of a carbon-based material, which confers the advantages of high power, and the other electrode realized with a material with faradic properties to reach high capacity and high energy. In asymmetric supercondensors both storage mechanisms occur simultaneously, but one of them will predominate over the other.

Another advanced approach to increase the energy density of a supercapacitor consists in functionalizing the materials for the carbon-based electrodes by adding electrochemically active materials. An alternative architecture for supercapacitors is given by placing the electrodes on the two sides of the substrate, thus manufacturing a two-sided structure where paper is used both as a substrate of the supecapacitor, as separator, and as a solid electrolyte, with consequent release of the electrons to the regenerative electrodes of the supercapacitor. In this type of devices, the porosity and hydrophilic character of the paper are considered an advantage, since they allow the absorption of the atmospheric agents, especially water vapor, triggering chemical reactions at the surface of the cellulose fibres. [159]

Ge et al. [141] reported an example of a hybrid supercapacitor made using a Kimwipess commercial paper (KIMTECH Sciencen brand delicate task wipers) characterized by macroporous cellulose fibres. In this case, paper was immersed first in a solution of single-walled carbon nanotubes (SWCNTs), which were wrapped around the cellulose fibres, and secondly, in a aniline solution where a polymerization step occurred. The resulting substrate was a hybrid electrode. Also the spacer here is based on paper which was immersed in (PVA) / H_3PO_4, wich acted as electrolyte. The final sandwich structure was obtained placing the paper soaked in the electrolyte between the two pieces of paper coated with SWCNT / PANI through lamination process. By connecting six supercapacitors of this type in series and charging them for 30 seconds, a voltage of 2.35V was obtained. The capacity of a SWCNT / PANI hybrid supercapacitor made in this way was 330 mF cm^{-2} while the capacities of an electrostatic supercapacitor (SWCNT) and a pseudo-capacitor (PANI) made with the same techniques are 46 mF cm^{-2} and 106 mF cm^{-2} respectively. These devices showed long life charge and discharge cycles (1000) with an excellent electrochemical stability even if curved or bent. The authors suggest that the durability can be further extended by introducing nanodiamonds into the SWCNT / PANI structure.

Limited energy capacities and densities were observed also by Kuzmenko et al. [143] for electrostatic supercapacitors with carbon nanofibre electrodes (CNF-electrodes). In this case the electrochemical performances of this device were improved by carbonization at 800 °C of the fibres of cellulose previously impregnated with double-wall carbon nanotubes (DWCNTs) or multi-wall carbon nanotubes (MWCNTs) to form composite electrodes CNF / DWCNT or CNF / MWCNT. The addition of CNT allows to increase the surface area of the electrodes, increasing the ability to accumulate charges and the electrical conductivity of the electrodes, thus ensuring a rapid charge transfer.

Considering electrodes realized with polymeric contacts, pseudo-capacitors with polypyrrole (PPy) electrodes realized using a polymerization process have been reported in the literature, delivering a capacity of 0.42 F cm^{-2}.[87] The same process applied to PEDOT:PSS electrodes led to a capacity of 85 mF cm^{-2}. The latter device was made on paper substrates with carbon fibres. An electrolyte gel ($BMIBF_4$) was spread between the electrodes to perform both the electrolyte and the separator role between the two electrodes. [142]

Ko et al. [43] reported the realization of electrodes using ligand-mediated assembly processes, in which the cellulose fibres are surrounded by metal oxides such as the hypomanganus oxide (MnO). The supercapacitor here was realized using a gel electrolyte between the two electrodes, leading to a symmetrical structure, with a capacity of 617 mF cm^{-2}. Realizing an alternating structure of MnO / Au bilayer the achievable capacity is 1.35 F cm^{-2}. In this case gold was used to increase the conductivity of the electrode, while the metal oxide to give the pseudo-capacitive behaviour.

A different approach in the realization of supercapacitors electrode is represented by the use of cellulose nanocrystals or bacterial cellulose to modify the properties of the substrate, and to make light, thin and transparent membranes to be used just as a substrate composed exclusively of cellulose. This approach allows to facilitate the self-assembly of the chemical species introduced in the successive deposition steps, thanks to the high density of hydroxyl side groups

(OH-) present on the surface of the substrate functionalized with cellulose or cellulose substrate. [5] An example of the functionalization of the surface with cellulose nanocrystals was reported by the work of Yang et al., in which the nanocrystals were impregnated on a substrate of Whatman filter paper, on which materials such as polypyrrole nanofibres (PPy-NF), polypyrrole with carbon nanotubes (PPy-CNT) or nanoparticles of manganese dioxide (MnO_2-NP) were deposited. Symmetric supercapacitors were realized using as a separator a porous polyethylene membrane containing a saturated solution of sodium sulfate (Na_2SO_4), which acts as aqueous electrolyte. Devices of this type had capacities per unit area of 3.32, 2.42 and 2.14 mF cm^{-2} (PPy-NF, PPy-CNT, MnO_2-NP) respectively .[145]

Bacterial cellulose has been also used as a membrane for the fabrication of electrodes. The process proposed by Peng et al. [146] foresees the dipping of cellulose in a copper acetate solution, to obtain a membrane covered with a copper oxide (CuO) layer on which the conductive polymeric species, such as for example polypyrrole (PPy) are then deposited. A symmetrical supercapacitor was realized using a spacer and an aqueous solution of sodium chloride (NaCl) as electrolyte. The addition of the copper oxide in this structure allowed to obtain better electrochemical characteristics of the electrode, allowing to reach a capacity of 601 Fg^{-1} with an energy density of 48.2 Wh kg^{-1} and a density in power of 85.8 W kg^{-1} at a current density of 0.8 mA cm^{-2}. [146]

A supercapacitor realized by inkjet printing technique was proposed by Liu et al. [144] They demonstrated the production of PEDOT / CNTs / Ag hybrid electrodes for a symmetrical supercapacitor. The electrolyte was composed of PVA / H_3PO_4 deposited by drop casting. The composition of the electrodes allows to form a 3D porous structure for an effective electrolyte transport and accessibility to the active site, obtaining a specific volume capacity of 23.6 F cm^{-3}. The processes for the realization and the performances of this device are schematically illustrated in **Figure 8**a and Figure 8b.

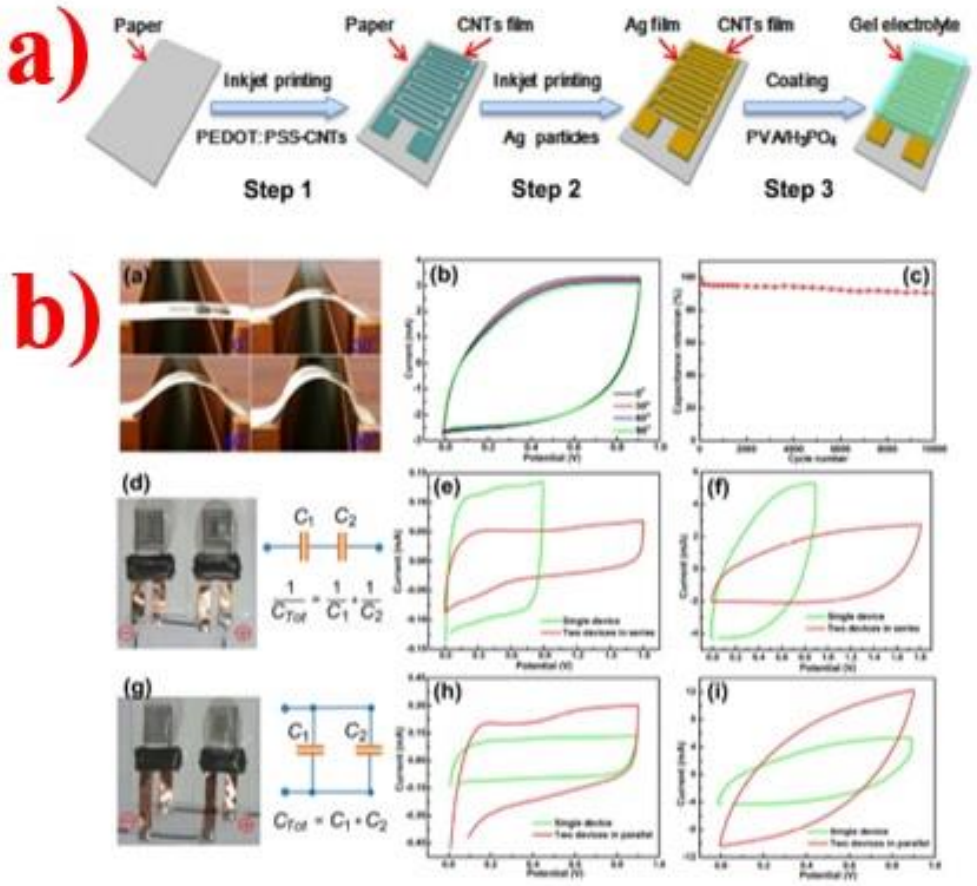

Figure 8: Symmetrical supercapacitor realized via inkjet printing: a) realization process b) electrical performances after bending tests. Reproduced with permission [144]. Copyright 2016, Journal of Materials Chemistry A.

5.2. Batteries on paper

Realization of paper based flexible batteries represents a very intriguing and challenging topic of research; so far, only few examples have been reported due to the technological issues that need to be overcome to prepare the different components of the device and to the assembling complexity on a flexible substrate (Table 4). Two main types of batteries have been realized so far on paper: electrochemical batteries (EB) and lithium based batteries (Lithium – ion batteries-LIB and Lithium-air Li-O_2). In the first case, the energy is generated through spontaneous redox reactions; the two electrodes are metals or conductive materials and in between them, there is

an ion exchange membrane or a salt bridge, which guarantees the correct behavior of the two electrodes and relative electrolytes, preventing the mixing of the solution and/or eventual side reactions. For this type of batteries, paper is used mainly as substrate for depositing electrodes or in its modified form as electrode itself, or as support for electrolytes. The first example of battery on paper, reported by Hilder et al.,[147] is an electrochemical zinc-air battery. Photo quality paper acted as support for the electrodes as well as reservoir for the electrolyte. The anode, realized with a zinc/carbon/polymer binder composite was air brushed on one side of the sheet, while on the other side a PEDOT layer is deposited using the inkjet printing of an oxidant followed by vapor phase polymerization.[160] The electrolyte LiCl/LiOH in aqueous solution was absorbed on the polymeric matrix. The resulting device showed a capacity of 0.5 mAh cm^{-2}. The authors ascribe such poor performances to the low performances of the paper-electrolyte system. Similar approach was reported by I.Ferreira et al.[149,150] In their work the electrodes were solid state films deposited via evaporation on two sides of a standard paper foil, which acted as support for them and also as reservoir for the electrolyte, that in this case was water. The cell battery was able to supply a $V_{OC} \cong 0.6$ V with a current density between 100 nA/cm^{-2} to 0.8 mA cm^{-2} and a power density between 75 nW cm^{-2} and 350 μW/cm^{-2}, for a relative humidity in the range of 60–85%.

Another approach to realize electrochemical batteries using paper was proposed by Nystrom et al.[148] In this case, filter paper acted as reservoir for the NaCl electrolyte; the two electrodes, realized using highly porous Cladophora cellulose coated with PPy composite in its oxidized and reduced form, were put in contact on one side with the paper and on the other side with platinum foils to collect charges. The whole system was then blocked with two microslides and packaged in a pouch, similar to the one used for LIB, to prevent the drying of the electrolyte (Figure 9a and Figure 9b). This type of devices showed a charge capacity of 50 mAh cm^{-2} with a very high stability in cycling behavior and a decrease of only 6% of the charge capacity after 100 cycles.

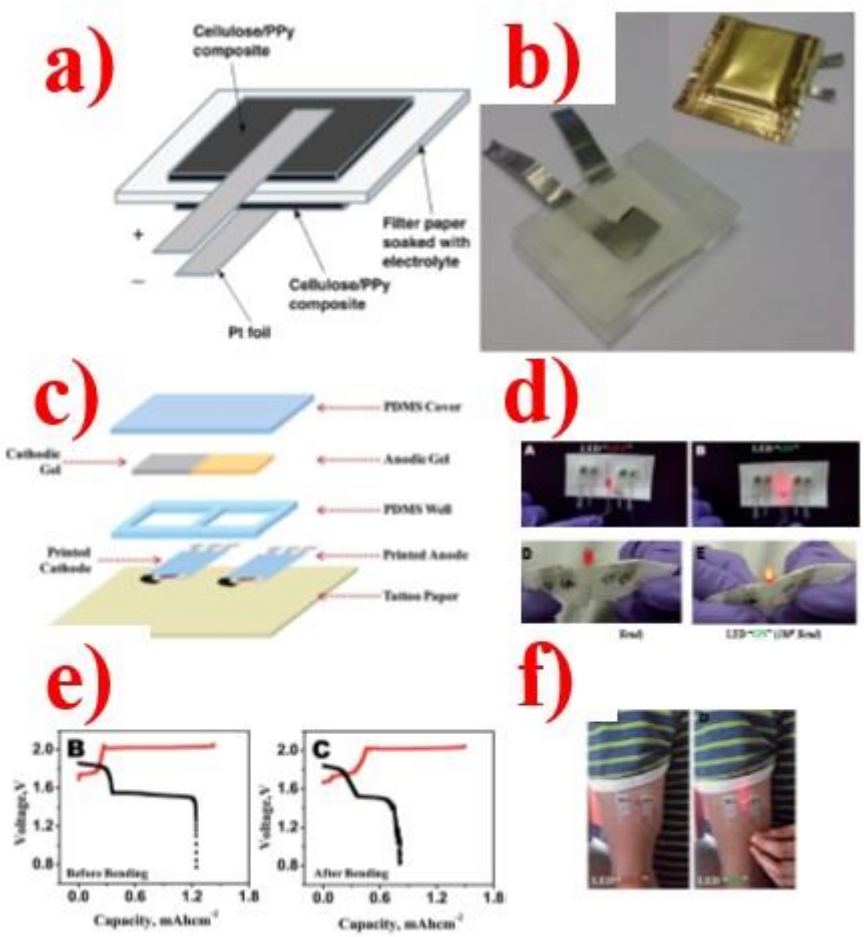

Figure 9. a) Schematic rappresentation of zinc-air battery and b) photograph of its final realization before and after sealing in aluminium pouch**.** Reproduced with permission [148]. Copyright 2009, American Chemical Society. c) Schematic digram of the realization steps of a Ag-Zn tattoo battery. d) Demonstration of the use of tattoo battery for LED lighting before and after stretching tests realized by bending the device 180° along the latitude for 100 cycles **.** e) Galvanostatic discharge capacity before and after stretching: the plot shows a decrease of 66% (red plot correspond to charging curves, black plots correspond to discharging curves). f) Demonstration of tattoo epidermal battery on skin. Reproduced with permission [153]. Copyright 2014, The Royal Society Chemistry.

A more unconventional approach was proposed by Berchmans et al.,[153] who realized an epidermal alkaline rechargeable Ag-Zn printable tattoo battery. In this device that is completely

flexible, printable and biocompatible, paper acts as a support for the screen-printed electrodes. The preparation process starts with the deposition on paper by screen printing of a transparent insulator, followed by an Ag layer as reference electrode and a carbon layer as current collector, on which Zn is electrodeposited. An additional semitransparent insulating layer was used to define the electrode active area. A polydimethylsiloxane (PDMS) well was deposited around the electrodes and filled with the anodic and cathodic gels; the gap between the electrodes wells was covered with an additional gel to guarantee the required ionic contact between the two electrodes (Figure 9c). The capacity shown by this device was 1.48 mAh cm^{-2}, which remained almost unchanged after 180 bending cycles (Figure 9d).

The second type of paper-based batteries is represented by lithium-ion batteries (LIB); the operating principle of these devices is based on the movement of lithium ions between the anode and the cathode through an electronically insulating, ion conducting electrolyte. The main characteristic of this type of batteries, which makes them attractive for many different applications, is represented by their high power and current density which make them the preferred type of batteries for powering high power electronics.[6] The main drawbacks of this type of devices are the complexity of the preparation process, which requires deposition of a multilayered structure, with high design complexity, and the use of high cost and non-environmentally friendly materials which require specific disposal procedures.

To date, flexible LIB realized with "paper-like" electrodes are the major focus of this research area[34,85] and only few papers reported devices realized using paper as constituent parts of the device. In particular Hu et al.[48] demonstrated the first LIB on paper realizing the two current collectors using carbon nanotubes deposited via manual Mayer rod coating on Xerox paper (Figure 10b). The two electrodes, divided by a separator, were coated with $LiMn_2O_4$ nanorods and $Li_4Ti_5O_{12}$ or SiC nanopowders to realize the anode and the cathode; $LiPF_6$ in ethylene carbonate/diethyl carbonate (EC/DEC) was used as electrolyte (Figure 10a). The device was assembled in a standard pouch cell. CNT coated paper showed a sheet resistance depending on

the thickness, which could reach values of 10 Ω/□ (Figure 10c). This system, used to power a blue LED (Figure 10e), demonstrated a capacity of 110 mAh g^{-1} and cycling stability of above 500 cycles (Figure 10d). The same group demonstrated a large area device where the CNTs film was a free standing membrane, with a sheet resistance of 5 Ω/□, realized by doctor blade coating, and paper was used as a spacer (Figure 10f-g). The device showed total capacity of 149 mAh g^{-1} and an energy density of 108 mWh g^{-1}.[154] More recently, they also demonstrated conductive nanopaper realized with cellulose nanofibres mixed with conductive nanotubes (CNTs) covered with silicon, deposited by plasma enhanced chemical vapour deposition (PECVD). These electrodes have been used as anodes in LIB showing for half cells a stable capacity of 1200 mAh g^{-1} for 100 cycles.[155]

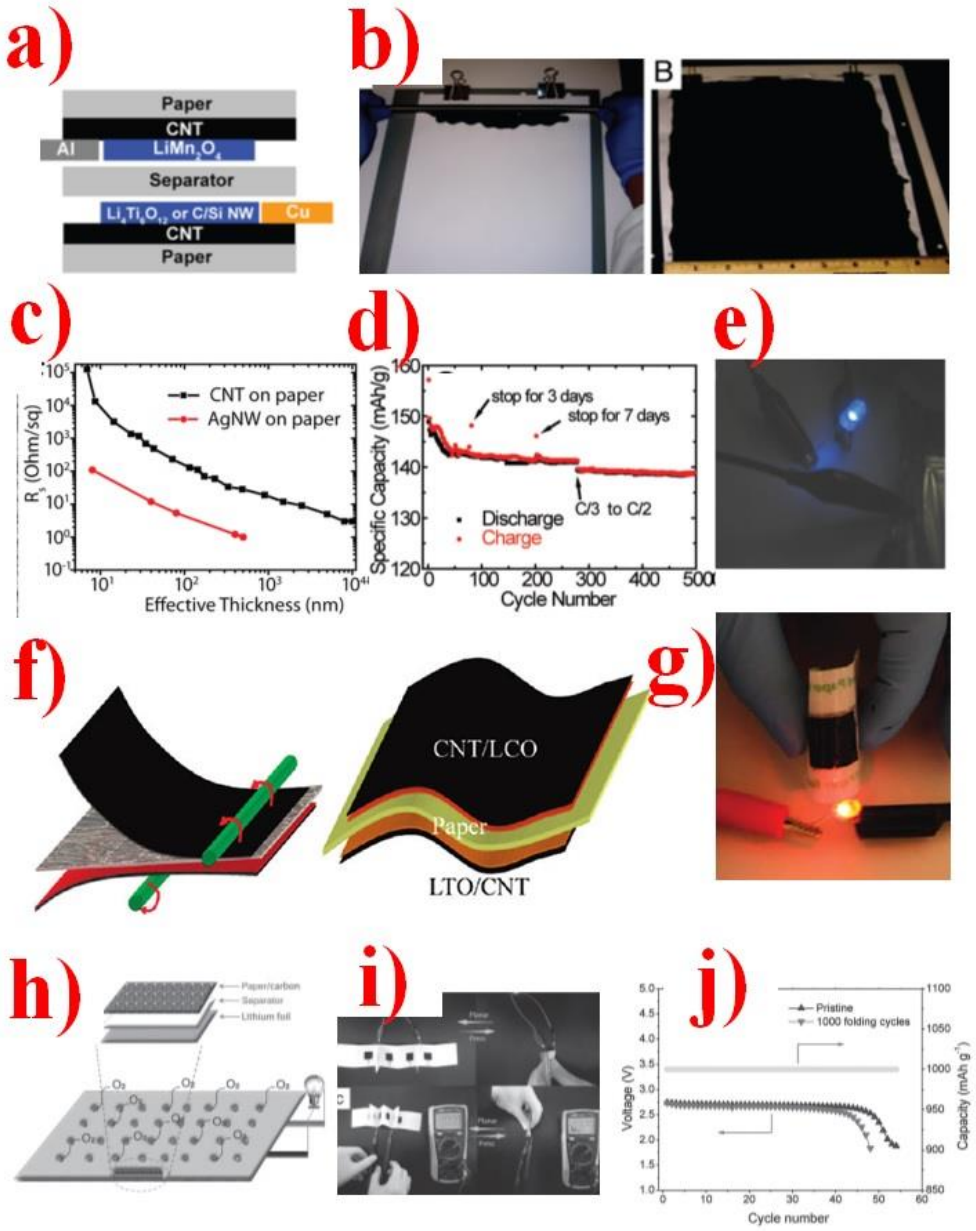

Figure 10. a) Schematic representation of LIB battery. b) Mayer rod coating of CNT paste on paper. c) Sheet resistance of CNTs and Ag nanowire films deposited with Mayer rod coating. d) Test on the stability of the battery: the capacity retention was 95% after 280 cycles at the rate of C/3. In the following 220 cycles at a rate of C/2 the battery showed a capacity decay of less than 0.01% per cycle. e) Flexible battery lighting a blue LED. Reproduced with permission [48]. Copyright 2009, Proceeding of the National Academy of Sciences of the United States of America. f) Schematic diagram of the of the lamination process of LIB. g) Flexible LIB lighting

a red LED[154] Copyright 2010, American Chemical Society. h) Schematic illustration of Li-O_2 battery assembly composed by a paper battery, a separator and a lithium foil. i) Photograph of Li-O_2 battery and measurement of the open circuit voltage. j) cycling performance of Li–O_2 batteries with pristine cathode and cathode after 1000 folding cycles with a fixed capacity of 1000 mAh g^{-1}. [156] Copyright 2015, Wyley-VCH

Lithium air batteries (Li-O_2) are particularly attractive with respect to LIB, as they can develop an extremely high energy density (3600 Wh Kg^{-1}), which is almost 10 times higher than conventional LIB. Very few examples of Li-O_2 batteries are reported in the literature and, to date, only one work, published by Liu et al., demonstrates a flexible and foldable Li-O_2 battery on paper.[156] Here the authors report on the realization of a carbon-based cathode using Chinese paint brush technique: carbon nanoparticles with a size of about 50 nm were deposited from solution on a standard paper substrate. After a drying process, the paper and the nanoparticles are tightly bonded together, demonstrating high electrical and mechanical stability. The foldable battery was then assembled using a glass fiber membrane, a lithium foil as anode and $LiCF_3SO_3$ in tetraethylene glycol dimethyl ether (TEGDME) as electrolyte. This device achieved a capacity of 6500 mAh g^{-1} for the cathode with high stability towards bending, able to maintain its performances almost unchanged after 1000 folding cycles. The full battery demonstrated a cycling lifetime of about 50 cycles with the capacity restricted to 1000 mAh g^{-1} at a current density of 200 mA g^{-1} (Figure 10 h-j).

6. Stability and Recycling.

6.1. Substrate and device stability

Only a limited number of reports have appeared so far considering the issue of shelf life of devices deposited on paper, and very few of them are relevant to solar cells and energy storage

devices supported on paper. However, mechanisms of degradation and the possible risks of exposure of paper to water and oxygen are known.

First and immediate problems are connected to paper structure and its interaction with humidity and solvents. In fact, paper is a web of fibres, therefore humidity and temperature variations may dramatically impact its morphology, influencing fibres aggregation, as well as their size and length.[161] Dimensional changes are normally reversible at low ambient humidity, but, above 65% humidity, they start to irreversibly affect the paper structure.[162] These morphological changes can impact any device operation[45] and adoption of a coating layer is beneficial for preserving contacts morphology, as demonstrated for printed silver linear electrodes on papers of different qualities subjected to cycles of exposure to humidity and thermal stress.[38] Improved dimensional stability was found for nanopaper containing up to 90 % of kaolin or precipitated calcium carbonate (PCC) fillers. Supercalendering improved the smoothness of the substrate.[72]

Furthermore, paper is bio-degraded by moulds, bacteria, and other organisms by means of enzymatic processes. The fungi Trichoderma reesei and Aspergillus niger attack paper producing extracellular enzymes called “cellulases”.[163] The main metabolite yielded by the action of cellulases is D-glucose, hence advanced degradation gives high free glucose content.[164] These attacks reduce the pH of paper and make it fragile: a decrease of cellulose degree of polymerization (DP) along with water infiltration modifies the interaction between fibres weakening paper cohesive interfibres bonds.[165] Oxidation of cellulose, performed through intervention of atmospheric oxygen and light, contributes to raising the concentration of acid in paper, since the primary alcohol groups in the cellulose polymer are turned to aldehyde group and later to carboxylic acid species. This could be a specific issue for paper photovoltaics, but at the moment no studies are reported on the influence of paper acidity on device stability and performances. Atmospheric pollutants, like inorganic oxides (NO_x or SO_x) can also contribute to paper degradation.[166] The expiration of a paper device essentially

depends on the time needed to degrade the cellulose, and this concept has been exploited, as highlighted in next paragraphs, to demonstrate the environmental sustainability of paper electronics.

Coating layers can be used to protect paper from degradation, which are also functional to preserving the active layers, when needed. For instance, an amount of 10 mg m^{-2} water reaching the organic layers can hamper the PCE of a solar cell of 50%,[167] and this can represent a problem considering that paper absorbs water during and after the different fabrication processes.[46] This, combined tot he high WVTR of cellulose paper leads a degradation of solar cell especially in organic and perovskite SCs. OPVs developed by Wang et al [46] displayed a loss of 50% of initial power conversion efficiency (PCE) after only 3.5h in air without encapsulation, 7 times faster than control references on glass. Among the protective layers proposed so far, parylene C, known for its excellent properties as permeation barrier, yielded very good results.[42] Barr et al [50] encapsulated the paper OPV with diverse techniques including lamination with a plastic film, and CVD deposition of Parylene C and a hydrophobic poly(1H,1H,2H,2H-perfluorodecyl acrylate) ("PPFDA") film. Although both CVD film were hydrophobic, the best encapsulation method, when samples were kept in air and constantly illuminated (80mW/cm^2), was the lamination which is also a low-cost and R2R compatible technique. Stability test of OPV module on paper are shown in **Figure 11**a): the laminated module retained the PCE for more than 500h. Figure 11b) shows the outstanding PCE of DSSC with a cellulose photoanode[103] after 1000h at 50ºC. The DSSC lost only 4% of its initial PCE (3.5%) after 1000h of stress. The stability of perovskite solar cells over a paper substrate was also gauged. Castro-Hermosa et al.[37] reported a fast decay of PCE after 72h of air exposure, while Jung et al.[57] showed that perovskite SC (see Figure 11c) retains 85% of initial PCE after 230h exposure in air. A PCE decay was attributed to $CH_3NH_3PbI_3$ degradation induced by external moisture or water content in paper substrate and possible degradation of the top contact.[57]

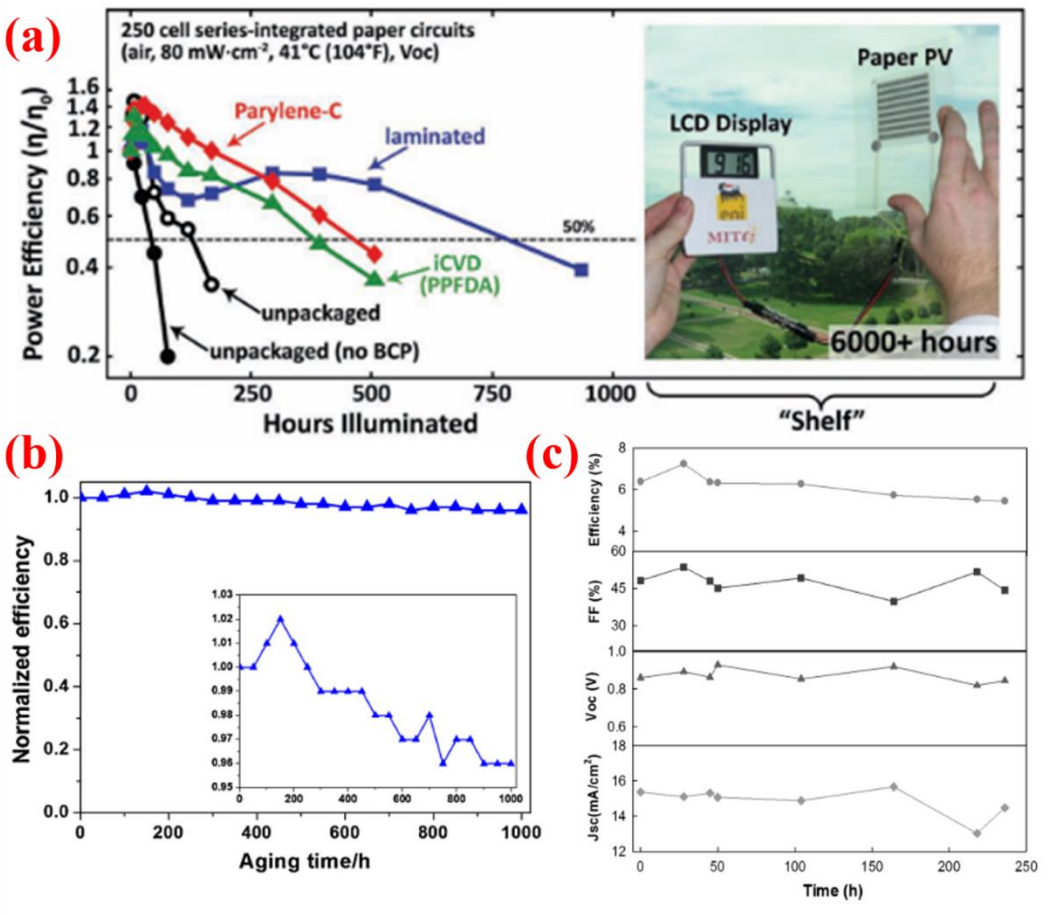

Figure 11. Long term stability of paper solar cells. (a) OPV module encapsulated with plastic lamination(blue), or CVD deposition of Paylene C (red) or PPFCA (green) films. Reproduced with permission.[50] Copyright 2011, John Wiley and Sons. Samples were kept in air at constant illumination (80mW/cm^2). (b) Long-term stability of DSSC with a cellulose photoanode at 50ºC in dark. Reproduced with permission.[103] Copyright 2017, Elsevier Ltd. All rights reserved. (c) Shel-life test of PSC on paper. Reproduced with permission.[57] Copyright 2016, Elsevier Ltd. All rights reserved.

A short-term stability, up to 3 weeks, was found for a low-voltage transistor with sorbitol-based ionic liquid as the electrolyte deposited on a biodegradable multicoated kaolin-based paper:[8] after this time water infiltration slowly caused the degradation of the device.[57] Encapsulation was shown to be necessary to preserve transistors from degradation when exposed to water

vapours.[38,39] Conversely, a barrier layer would not be advantageous in CNTs based supercapacitors: CNTs functionalized Xerox paper revealed better performances and stability than PET with the same functionalization, since the CNTs layer is easily peeled off from PET, while it sticks much more strongly on paper surface, yielding devices with high operational stability.[48] In this case, only encapsulation of the device would be necessary.

6.2. Disposal, recycling and environmental impact

The main advantages of investing in paper for electronics and energy storage devices reside in four main perspectives: (i) the low cost of the technology, (ii) the potentiality to recover devices components and recycle the substrate as well as the active materials; the production of (iii) environmentally harmless and (iv) biocompatible devices. The first advantage has been widely discussed in the previous paragraphs, highlighting also the present availability of scalable printing techniques. The remaining three still need to receive an in-depth study; however, some research is already published on these subjects, especially regarding the environmental harmlessness of paper, which is actually its most important property.

6.2.1 Recycling of paper

Recyclability is demonstrated for standard paper: it consists in recovering cellulose fibres from waste paper, by separating them from all the impurities. The waste paper is grinded into a mill and re-converted into a pulp, which is forced through a series of screens with apertures of diverse dimension and shapes to separate materials by their size; in this way, while the heavier elements may be separated letting them sediment at the bottom of the re-pulper, it is possible to remove small contaminants such as bits of plastic and globs of glue. However, accurate washing from contaminants is necessary prior to milling. Typical contaminants are adhesives, resins, waxes and fillers (like calcium carbonate or titanium dioxide).[168]

In the case of printed paper, standard inks are removed by treatment in a chemical or enzymatic bath and subsequent water washing or flotation. In flotation, a soap is introduced in the re-pulper for air-bubbling; hydrophobic inks stick to and are mechanically transported on top of

the re-pulper by air bubbles, while the pulp is poured in a screening machine. As chemical method, saponification represents a good strategy to erase many oil-based prints; while enzymatic treatment may involve cellulases, that removes surface fibres, or lipases, to remove oily inks. The main inconvenience is usually given by ageing of the printed paper, that makes ink removal more difficult.[2]

A proof-of-concept of device recycling was published with nanopaper used as the substrate. For a polymer solar cell with inverted geometry deposited on transparent nanopaper, at the end of the device lifetime, a sequence of different solvents was used to recover the different materials: distilled water can dissolve the nanopaper in 30 minutes; after that, chlorobenzene can dissolve the organic layers, previously recovered by filtration; finally, the Ag contacts are recovered as well by filtration (**Figure 12**a).[61] However, it is very hard to imagine that a nanopaper dissolved by water in 30 minutes may find commercial application in the field of paper electronics. The nanopaper published in the article by Zhou et al. was prepared by solution casting cellulose nanocrystals. Operamolla et al.[67] showed fast kinetic of water uptake by means of electrochemical studies on a nanopaper prepared by drop-cast method. Conversely, chemical functionalization of the nanopaper yielded much more stable and versatile thin films. More compact and dimensionally stable nanopaper than the one presented by Zhou et al. may be attained by applying standard machine processing of papermaking with the aid of vacuum-hot presses [55] and applying chemical modification treatments,like blending nanocellulose with cellulose derivatives [70] or performing a surface functionalization to increase the hydrophobic[57,66,67] or amphiphobic character of the nanopaper.

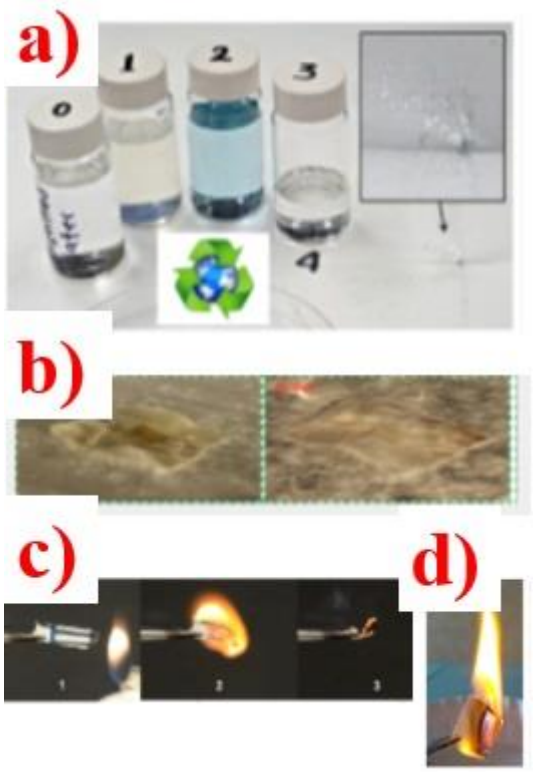

Figure 12. a) Results of the recycling of an organic solar cell deposited on nanopaper: vial 1 – distilled water; vial 2 – CNCs re-dispersed in water; vial 3 and vial 4 – rinsing solutions in chlorobenzene of organic layers; 4 and inset: metallic contacts (Ag and MoO3). Reproduced with permission.[62] Copyright 2013, Springer Nature. All rights reserved. b) Photographs of a nanopaper-based electronics after 10 days and 60 days of degradation by Postia placenta. The fungus fully covers the film after 60 days. Reproduced with permission.[22] Copyright 2015, Springer Nature. All rights reserved. c) Different frames of an organic solar cell deposited on nanopaper incineration. Reproduced with permission.[61] Copyright 2013, Springer Nature. All rights reserved. d) Incineration of a perovskite solar cell deposited on PowerCoat. Reproduced with permission.[37] Copyright 2017, IEEE. All rights reserved.

6.2.2 Recycling of device active layers

A general reliable recycling method for printed devices has not been formulated yet. This represents quite an open issue, since the recycling of paper requires paper cleaning and there is not, at the moment, a standard method to recover and recycle devices active layers. Moreover,

paper recycling may present some issues: mixing different qualities of paper in the recycling process does not commonly represent an advantage as, for instance, newspapers should not be mixed with magazines or boxes, and so on. Consequently, it would be needed either (i) to focus on one quality of paper only for developing the entire paper electronics market or (ii) dispose devices separating them based on the kind of paper. For this reason, a valuable alternative consists in the use of natural methods for degradation of the paper component of the devices and the recovery and recycling of the more precious active layers. In this way, only the cheapest part of the printed electronic devices would be lost. For example, fungal degradation was used to demonstrate biodegradability of CNF- nanopaper used as substrate in GaAs electronic circuits. As presented in Figure 12b), the fungi only partially covered the sample after 10 days but were able to fully cover it after 60 days. Once degraded, the leftover electronics portion, which is protected by polyimide barrier layers, non-permeable to water or solvents and working as a protection layer against any leakage of materials to the environment, can be collected to be further decomposed and recycled.[22]

6.2.3 Environmental harmlessness and biocompatibility

The accidental release of a device deposited on paper should not negatively impact the environment: this objective can be pursued by using substrates composed by completely biodegradable components, ensuring environmentally friendly disposal, composting and incineration of the materials. Some coating materials, like plastics, organometallics or metal oxides, are clearly not biodegradable or can even be toxic. Conversely, some of the most recent coating strategies that have been developed are carried out by using sustainable and biodegradable starting materials [8,37,73,38,39,46,47,49,66,67,70]. In most cases, the method proposed for the easy disposal of the devices at the end of their lifetime is incineration, that would destroy the organic material. Figure 12 demonstrates this strategy applied to organic and perovskite solar cells deposited on nanopaper[61] and PowerCoat[37] paper, respectively. In the case of the perovskite solar cell, Pb could be recovered from ashes. Some composite papers, like TEMPO

transparent paper or cellulose nanofibres/cellulose ethers paper are also declared to be sustainable and biodegradable after service.[47]

Fully disintegrable transient devices (OFETs), with a harmlessness active layer, were produced on a biodegradable ultrathin (800 nm) substrate based on regenerated cellulose for ultra-lightweight (2 g/m^2) electronics. The devices yielded complete disintegration after 30 days of exposure to mild acidic conditions.[74] Biodegradability was also demonstrated for a battery deposited on paper.[44] The battery was composed only of organic materials (cellulose, carbon, wax and an integrated quinone redox couple). Device components were non-toxic and showed to be biotically degradable in a standardized test. Nanopaper, as standard paper, is biodegradable by fungi as well.[22] Moreover, nanocrystalline celluloses are commonly perceived as non-toxic, specifically in case of ingestion and dermal contact,[169] and some studies demonstrating their safety and biocompatibility, also including tolerance and rapid excretion from mammalian body[170] are in progress, signifying the high potentialities of nanopaper as substrate for electronics and as point-of-care platform, with possible implications in drug delivery- or health monitor systems.

7. Conclusions and perspectives

In the past years, a great deal of interest has been given to flexible power sources for powering the new generation of flexible and wearable electronic devices and systems. In this context, paper based solar cells, supercapacitors and batteries represent a new class of devices that are attracting more and more attention from the scientific community due to the ease of processing, which is compatible with roll to roll fabrication techniques and to the possibility of achieving flexible, low-weight, biocompatible, easily recyclable devices with potentially low environmental impact. In this review, the recent advances in printed solar cells, supecapacitors and batteries fabricated on paper substrates were reviewed. Special emphasis was given to the analysis of the substrate characteristics required to achieve high performance devices focussing

on the role of surface treatments as well as on the possibility of forming cellulose based composites with specific characteristics such as transparency, better wettability, and durability. The main printing techniques implemented for the two types of technologies were reported highlighting the impact of parameters such as R2R compatibility, material waste and layer thickness on the manufacturing processes.

In case of printed solar cells on paper, a detailed review on the type of electrodes, semi-transparent or opaque, as well as on the different type of photovoltaic technologies fabricated on paper were described evidencing not only the performances, but also the stability measured so far. Solar cells with efficiencies of up to ~ 4% on opaque substrates and 9% on transparent substrates have been demonstrated and reported. As for the storage devices, recent advances in the fabrication process and the potential applications of paper supercapacitor and batteries on paper were detailed focussing mainly on the architecture proposed so far, on their construction and on the role of different types of electrodes studied to improve device performance. In this case, supercapacitors and batteries with maximum achieved capacity of 1350 mF cm^{-2} and 6500 mAh g^{-1} respectively are reported.

Stability and recyclability issues were also considered evidencing how the substrate plays a fundamental role in both aspects; if, in fact, it can be a major contributor affecting degradation and the overall lifetime of the devices, on the other side it allows a quite easy recyclability.

Analyzing the literature, it becomes apparent that several aspects still need to be solved to achieve long lifetime and high performing devices able to power the future generation flexible devices on paper. In particular, for the substrate even though several coatings have been studied to smoothen the paper surface and to increase the durability, stability is still an open issue. Very limited number of manuscripts report on shelf life of devices deposited on paper, and the impact of humidity, temperature, as well as the action of moulds, bacteria, other organisms and pollution on the paper degradation are still under study and have not been directly correlated with the lifetime of solar cells and storage devices.

Boosting the performances in terms of available power of both type of devices is of a paramount importance for their effective application in flexible paper based electronics. The commercialization of such devices will require a design and fabrication process that are easy to transfer to a roll to roll system. Printing process would allow customized generation and harvesting systems, which could even be integrated together to realize a rechargeable autonomous supply system. However, while in the case of solar cells existing printing processes implemented on flexible plastic substrates can be adapted to paper substrates in the future, for supercapacitors and batteries it could be a bit more challenging as it would require high performing printed electrolytes and flexible packaging systems.

The development of a thin, flexible packaging, which is impermeable to moisture and prevent the leak and degradation of the electrolyte, would be a fundamental step for making flexible storage systems, particularly lithium batteries, more compliant to printable electronics for the possibility to integrate them on flexible substrates and also for safety reasons. Standard pouches used in labs are in fact made with aluminum foils 125 μm thick, which can be hardly integrated on flexible substrates. Examples of pouches based on PDMS or elastomers have been reported, but still have a high permeation rate of moisture. Packaging would play a fundamental role also in case of solar cells, as it would guarantee longer stability and lifetime.

In terms of recyclability, while some manuscripts already discuss how to reuse paper and nanopaper by removing contaminants such as adhesive, resins, waxes and fillers, no standard reliable process to recycle the active parts of the devices on paper has been formulated yet. Therefore this is a fundamental open issue to be investigated to properly evaluate the overall sustainability of the production of these devices.

Potential applications, when the various technical issues described can be effectively addressed, are two fold. Firstly, the single type of devices highlighted here can be inserted individually in common commercial products. It is likely that the most promising sector for initial markets will be that of paper batteries and supercapacitors. In fact, power capacitors based on paper are

already in use in applications such as utility poles. The versatility in being able to adapt to different forms and shapes should open up their insertion in many future product markets.[171] Secondly, the more exciting and futuristic potential, is that of being integrated with other printed electronics (in order to power the electronic functionality) as well as graphics on paper substrates. The range of potential products can be staggering: smart labels, smart ticketing, novelty cards, smart packaging, disposable packaging and radiofrequency identification tags for inventory management or food labels[172], disposable chemical, or biomedical sensors, single-use diagnostic devices, even wearable sensors in healthcare. Further applications can be envisaged in security, safety, crime prevention, anti-counterfeiting, brand enhancement and merchandising, simple display and signage sectors. [173] The low environmental impact (for example that of paper-based multilayer printed circuit boards is two orders of magnitude lower that of currently available organic PCBs [174]) and cost of paper as well as its recyclability will play a big role in its commercial appeal and uptake. Paper has the potential to extend the reach of electronics into new markets which have not been considered before.[175]

Acknowledgements

This work was supported by the Departamento del Huila's Scholarship Program No. 677 from Huila, Colombia. AO acknowledges Regione Puglia, program FutureInResearch, project ''SolarLeaf – Biodegradable organic solar cells supported on cellulose (Prot. F6YRA01)'' and Università degli Studi di Bari Aldo Moro. FB and TMB acknowledge the European H2020 project, "Wearable Applications enabled by electronic Systems on Paper (WASP)" (no. 825213). TMB acknowledges the University of Rome Tor Vergata's "Mission: Sustainability" "BiCVision" project and LazioInnova research project n. 85-2017-15373 – "Sight Restoration via Organic and Hybrid Thin Films (SIROH)".

Received: ((will be filled in by the editorial staff))
Revised: ((will be filled in by the editorial staff))
Published online: ((will be filled in by the editorial staff))

References

[1] Data from CEPI, RISI, AF&PA, JPA, PPPC, Bracelpa. Source: Assocarta website, www.assocarta.it **2015**.

[2] C. J. Biermann, *Handbook of Pulping and Papermaking*; 1996.

[3] H. Zhu, Z. Fang, C. Preston, Y. Li, L. Hu, *Energy Environ. Sci.* **2014**, *7*, 269.

[4] H. Águas, T. Mateus, A. Vicente, D. Gaspar, M. J. Mendes, W. A. Schmidt, L. Pereira, E. Fortunato, R. Martins, *Adv. Funct. Mater.* **2015**, *25*, 3592.

[5] R. J. Moon, A. Martini, J. Nairn, J. Simonsen, J. Youngblood, *Cellulose nanomaterials review: Structure, properties and nanocomposites*; 2011; Vol. 40.

[6] T. H. Nguyen, A. Fraiwan, S. Choi, *Biosens. Bioelectron.* **2014**, *54*, 640.

[7] B. S. Irimia-Vladu M., Glowacki E. D., Sariciftci N. S., *Green Materials for Electronics*; Wiley-VCH Verlag GmbH & Co. KGaA., 2018.

[8] R. Bollström, A. Määttänen, D. Tobjörk, P. Ihalainen, N. Kaihovirta, R. Österbacka, J. Peltonen, M. Toivakka, *Org. Electron. physics, Mater. Appl.* **2009**, *10*, 1020.

[9] A. Hübler, B. Trnovec, T. Zillger, M. Ali, N. Wetzold, M. Mingebach, A. Wagenpfahl, C. Deibel, V. Dyakonov, *Adv. Energy Mater.* **2011**, *1*, 1018.

[10] A. Barhoum, P. Samyn, T. Öhlund, A. Dufresne, *Nanoscale* **2017**, *9*, 15181.

[11] D. Tobjörk, R. Österbacka, *Adv. Mater.* **2011**, *23*, 1935.

[12] Bacon W.S., *Pop. Sci. Mag.* **1968**, 124.

[13] T. P. Brody, *Radio Electron. Eng.* **1969**, *38*, 326.

[14] T. Peter Brody, *IEEE Trans. Electron Devices* **1984**, *31*, 1614.

[15] S. Thiemann, S. J. Sachnov, F. Pettersson, R. Bollström, R. Österbacka, P. Wasserscheid, J. Zaumseil, *Adv. Funct. Mater.* **2014**, *24*, 625.

[16] D. H. Lien, Z. K. Kao, T. H. Huang, Y. C. Liao, S. C. Lee, J. H. He, *ACS Nano* **2014**, *8*, 7613.

[17] F. Shao, P. Feng, C. Wan, X. Wan, Y. Yang, Y. Shi, Q. Wan, *Adv. Electron. Mater.* **2017**, *3*, 1.

[18] K. H. Choi, D. B. Ahn, S. Y. Lee, *ACS Energy Lett.* **2018**, *3*, 220.

[19] H. Zhu, Z. Xiao, D. Liu, Y. Li, N. J. Weadock, Z. Fang, J. Huang, L. Hu, *Energy Environ. Sci.* **2013**, *6*, 2105.

[20] Y. Yao, J. Tao, J. Zou, B. Zhang, T. Li, J. Dai, M. Zhu, S. Wang, K. K. Fu, D. Henderson, E. Hitz, J. Peng, L. Hu, *Energy Environ. Sci.* **2016**, *9*, 2278.

[21] A. Paul, M. A. Kafi, R. Dahiya, *Proc. IEEE Sensors* **2017**, *2017–Decem*, 17.

[22] Y. H. Jung, T.-H. Chang, H. Zhang, C. Yao, Q. Zheng, V. W. Yang, H. Mi, M. Kim, S. J. Cho, D.-W. Park, H. Jiang, J. Lee, Y. Qiu, W. Zhou, Z. Cai, S. Gong, Z. Ma, *Nat. Commun.* **2015**, *6*, 7170.

[23] R. Martins, D. Gaspar, M. J. Mendes, L. Pereira, J. Martins, P. Bahubalindruni, P. Barquinha, E. Fortunato, *Appl. Mater. Today* **2018**, *12*, 402.

[24] L. Pereira, D. Gaspar, D. Guerin, L. M. Castano, A. B. Flatau, H. A. Andersson, A. Manuilskiy, S. Haller, K. Torvinen, F. Pettersson, P. Lahtinen, L. Y. Xu, G. Y. Yang, H. Y. Jing, S. Kim, H. W. Kang, K. H. Lee, S. Kanaparthi, S. Badhulika, R. Barras, I. Cunha, E. Fortunato, R. Martins, D. Gaspar, E. Fortunato, R. Martins, L. Pereira, *Flex. Print. Electron.* **2017**, *2*, 014006.

[25] R. Barras, I. Cunha, D. Gaspar, E. Fortunato, R. Martins, L. Pereira, *Flex. Print. Electron.* **2017**, *2*.

[26] J. M. Nassar, K. Mishra, K. Lau, A. A. Aguirre-Pablo, M. M. Hussain, *Adv. Mater. Technol.* **2017**, *2*, 1.

[27] X. Du, Z. Zhang, W. Liu, Y. Deng, *Nano Energy* **2017**, *35*, 299.

[28] F. Sharifi, S. Ghobadian, F. R. Cavalcanti, N. Hashemi, *Renew. Sustain. Energy Rev.*

2015, *52*, 1453.

[29] D. Ha, Z. Fang, N. B. Zhitenev, *Adv. Electron. Mater.* **2018**, *4*, 1.

[30] H. Liu, H. Qing, Z. Li, Y. L. Han, M. Lin, H. Yang, A. Li, T. J. Lu, F. Li, F. Xu, *Mater. Sci. Eng. R Reports* **2017**, *112*, 1.

[31] S. Razza, S. Castro-Hermosa, A. Di Carlo, T. M. Brown, *APL Mater.* **2016**, *4*, 091508.

[32] A. M. Gaikwad, A. C. Arias, D. A. Steingart, *Energy Technol.* **2014**, *3*, 305.

[33] R. E. Sousa, C. M. Costa, S. Lanceros-Méndez, *ChemSusChem* **2015**, *8*, 3539.

[34] B. Yao, J. Zhang, T. Kou, Y. Song, T. Liu, Y. Li, *Adv. Sci.* **2017**, *4*.

[35] L. Leonat, M. S. White, E. D. Glowacki, M. C. Scharber, T. Zillger, J. Rühling, A. Hübler, N. S. Sariciftci, *J. Phys. Chem. C* **2014**, *118*, 16813.

[36] A. H. Bedane, M. Eić, M. Farmahini-Farahani, H. Xiao, *Cellulose* **2016**, *23*, 1537.

[37] S. Castro-Hermosa, J. Dagar, A. Marsella, T. M. Brown, *IEEE Electron Device Lett.* **2017**, *38*, 1278.

[38] R. Bollström, F. Pettersson, P. Dolietis, J. Preston, R. Österbacka, M. Toivakka, *Nanotechnology* **2014**, *25*.

[39] F. Pettersson, D. Adekanye, R. Österbacka, *Phys. Status Solidi Appl. Mater. Sci.* **2015**, *212*, 2696.

[40] L. Ren'Ai, K. Zhang, G. Chen, B. Su, J. Tian, M. He, F. Lu, *Chem. Commun.* **2018**, *54*, 2304.

[41] M. He, K. Zhang, G. Chen, J. Tian, B. Su, *ACS Appl. Mater. Interfaces* **2017**, *9*, 16466.

[42] B. Lamprecht, R. Thünauer, M. Ostermann, G. Jakopic, G. Leising, *Phys. Status Solidi Appl. Mater. Sci.* **2005**, *202*, 50.

[43] Y. Ko, M. Kwon, W. K. Bae, B. Lee, S. W. Lee, J. Cho, *Nat. Commun.* **2017**, *8*, 1.

[44] J. P. Esquivel, P. Alday, O. A. Ibrahim, B. Fernández, E. Kjeang, N. Sabaté, *Adv. Energy Mater.* **2017**, *7*.

[45] S. A. Shenton, M. D. Cooke, Z. Racz, C. Balocco, D. Wood, *Phys. Status Solidi Appl.*

Mater. Sci. **2018**, *215*, 1.

[46] F. Wang, Z. Chen, L. Xiao, B. Qu, Q. Gong, *Sol. Energy Mater. Sol. Cells* **2010**, *94*, 1270.

[47] H. Fang, J. Li, J. Ding, Y. Sun, Q. Li, J. L. Sun, L. Wang, Q. Yan, *ACS Appl. Mater. Interfaces* **2017**, *9*, 10921.

[48] L. Hu, J. W. Choi, Y. Yang, S. Jeong, F. La Mantia, L.-F. Cui, Y. Cui, *Proc. Natl. Acad. Sci.* **2009**, *106*, 21490.

[49] W. Hu, G. Chen, Y. Liu, Y. Liu, B. Li, Z. Fang, *ACS Sustain. Chem. Eng.* **2018**, *6*, 6974.

[50] M. C. Barr, J. A. Rowehl, R. R. Lunt, J. Xu, A. Wang, C. M. Boyce, S. G. Im, V. Bulović, K. K. Gleason, *Adv. Mater.* **2011**, *23*, 3500.

[51] Z. Fang, H. Zhu, Y. Yuan, D. Ha, S. Zhu, C. Preston, Q. Chen, Y. Li, X. Han, S. Lee, G. Chen, T. Li, J. Munday, J. Huang, L. Hu, *Nano Lett.* **2014**, *14*, 765.

[52] T. Nishino, N. Arimoto, *Biomacromolecules* **2007**, *8*, 2712.

[53] P. Phanthong, G. Guan, S. Karnjanakom, X. Hao, Z. Wang, K. Kusakabe, A. Abudula, *RSC Adv.* **2016**, *6*, 13328.

[54] Z. Weng, Y. Su, D. W. Wang, F. Li, J. Du, H. M. Cheng, *Adv. Energy Mater.* **2011**, *1*, 917.

[55] M. Nogi, S. Iwamoto, A. N. Nakagaito, H. Yano, *Adv. Mater.* **2009**, *21*, 1595.

[56] L. Hu, G. Zheng, J. Yao, N. Liu, B. Weil, M. Eskilsson, E. Karabulut, Z. Ruan, S. Fan, J. T. Bloking, M. D. McGehee, L. Wågberg, Y. Cui, *Energy Environ. Sci.* **2013**, *6*, 513.

[57] M.-H. Jung, N.-M. Park, S.-Y. Lee, *Sol. Energy* **2016**, *139*, 458.

[58] H. Zhu, L. Hu, J. Cumings, J. Huang, Y. Chen, *ACS Nano* **2013**, 2106.

[59] S. V. Costa, P. Pingel, S. Janietz, A. F. Nogueira, *J. Appl. Polym. Sci.* **2016**, *133*, 6.

[60] Y. Fujisaki, H. Koga, Y. Nakajima, M. Nakata, H. Tsuji, T. Yamamoto, T. Kurita, M. Nogi, N. Shimidzu, *Adv. Funct. Mater.* **2014**, *24*, 1657.

[61] Y. Zhou, C. Fuentes-Hernandez, T. M. Khan, J.-C. Liu, J. Hsu, J. W. Shim, A. Dindar, J. P. Youngblood, R. J. Moon, B. Kippelen, *Sci. Rep.* **2013**, *3*, 1536.

[62] Y. Zhou, T. M. Khan, J. C. Liu, C. Fuentes-Hernandez, J. W. Shim, E. Najafabadi, J. P. Youngblood, R. J. Moon, B. Kippelen, *Org. Electron. physics, Mater. Appl.* **2014**, *15*, 661.

[63] M. Nogi, M. Karakawa, N. Komoda, H. Yagyu, T. T. Nge, *Sci. Rep.* **2015**, *5*, 1.

[64] J. Tao, Z. Fang, Q. Zhang, W. Bao, M. Zhu, Y. Yao, Y. Wang, J. Dai, A. Zhang, C. Leng, D. Henderson, Z. Wang, L. Hu, *Adv. Electron. Mater.* **2017**, *3*, 1.

[65] Z. Yu, Z. Xu, K. Qiao, L. Zhang, Z. Chen, X. Yang, A. Ji, M. Wu, Y. Gao, *Macromol. Mater. Eng.* **2018**, *303*, 1.

[66] A. G. Cunha, Q. Zhou, P. T. Larsson, L. A. Berglund, *Cellulose* **2014**, *21*, 2773.

[67] A. Operamolla, S. Casalini, D. Console, L. Capodieci, F. Di Benedetto, G. V. Bianco, F. Babudri, *Soft Matter* **2018**, *14*, 7390.

[68] and F. W. Kezheng Gao, Ziqiang Shao, Xue Wu, Xi Wang, Yunhua Zhang, Wenjun Wang, *Nanoscale* **2013**.

[69] A. Hajian, S. B. Lindström, T. Pettersson, M. M. Hamedi, L. Wågberg, *Nano Lett.* **2017**, *17*, 1439.

[70] Q. Cheng, D. Ye, W. Yang, S. Zhang, H. Chen, C. Chang, L. Zhang, *ACS Sustain. Chem. Eng.* **2018**.

[71] S. Chen, Y. Song, F. Xu, *ACS Sustain. Chem. Eng.* **2018**, *6*, 5173.

[72] K. Torvinen, J. Sievänen, T. Hjelt, E. Hellén, *Cellulose* **2012**, *19*, 821.

[73] Y. Su, Y. Zhao, H. Zhang, X. Feng, L. Shi, J. Fang, *J. Mater. Chem. C* **2017**, *5*, 573.

[74] T. Lei, M. Guan, J. Liu, H.-C. Lin, R. Pfattner, L. Shaw, A. F. McGuire, T.-C. Huang, L. Shao, K.-T. Cheng, J. B.-H. Tok, Z. Bao, *Proc. Natl. Acad. Sci.* **2017**, *114*, 5107.

[75] A. T. Vicente, A. Araújo, M. J. Mendes, D. Nunes, M. J. Oliveira, O. Sanchez-Sobrado, M. P. Ferreira, H. Águas, E. Fortunato, R. Martins, *J. Mater. Chem. C* **2018**,

6, 3143.

[76] F. B. A. Operamolla, S. Casalini, D. Console, L. Capodieci, F. Di Benedetto, G. Valerio Bianco, **2018**, *Submitted*.

[77] L. Hu, Y. Cui, *Energy Environ. Sci.* **2012**, *5*, 6423.

[78] F. C. Krebs, *Sol. Energy Mater. Sol. Cells* **2009**, *93*, 394.

[79] F. Di Giacomo, A. Fakharuddin, R. Jose, T. M. Brown, *Energy Environ. Sci.* **2016**, *9*, 3007.

[80] T. Tao, S. Lu, Y. Chen, *Adv. Mater. Technol.* **2018**.

[81] L. Jabbour, R. Bongiovanni, D. Chaussy, C. Gerbaldi, D. Beneventi, *Cellulose* **2013**, *20*, 1523.

[82] G. Cummins, M. P. Y. Desmulliez, *Circuit World* **2012**, *38*, 193.

[83] S. Khan, L. Lorenzelli, R. S. Dahiya, *IEEE Sens. J.* **2015**, *15*, 3164.

[84] R. Abbel, Y. Galagan, P. Groen, *Adv. Eng. Mater.* **2018**, *1701190*, 1.

[85] K. H. Choi, D. B. Ahn, S. Y. Lee, *ACS Energy Lett.* **2018**, *3*, 220.

[86] R. Søndergaard, M. Hösel, D. Angmo, T. T. Larsen-Olsen, F. C. Krebs, *Mater. Today* **2012**, *15*, 36.

[87] L. Yuan, B. Yao, B. Hu, K. Huo, W. Chen, J. Zhou, *Energy Environ. Sci.* **2013**, *6*, 470.

[88] Y. Galagan, R. Andriesse, In *Third Generation Photovoltaics, Organic photovoltaics: Technologies and manufacturing*; Fthenakis, V., Ed.; InTech, 2012.

[89] M. Sygletou, C. Petridis, E. Kymakis, E. Stratakis, *Adv. Mater.* **2017**, *29*, 1700335.

[90] G. Mincuzzi, A. L. Palma, A. Di Carlo, T. M. Brown, *ChemElectroChem* **2016**, *3*, 9.

[91] M. Morales-Masis, S. De Wolf, R. Woods-Robinson, J. W. Ager, C. Ballif, *Adv. Electron. Mater.* **2017**, *3*.

[92] E. Fortunato, D. Ginley, H. Hosono, D. C. Paine, *MRS Bull.* **2007**, *32*, 242.

[93] W. J. Scheideler, J. Smith, I. Deckman, S. Chung, A. C. Arias, V. Subramanian, *J. Mater. Chem. C* **2016**, *4*, 3248.

[94] Q. Xu, T. Song, W. Cui, Y. Liu, W. Xu, S. T. Lee, B. Sun, *ACS Appl. Mater. Interfaces* **2015**, *7*, 3272.

[95] R. A. Hatton, N. P. Blanchard, L. W. Tan, G. Latini, F. Cacialli, S. R. P. Silva, *Org. Electron. physics, Mater. Appl.* **2009**, *10*, 388.

[96] M. S. Tyler, M. Walker, R. A. Hatton, *ACS Appl. Mater. Interfaces* **2016**, *8*, 12316.

[97] L. Cattin, E. Jouad, N. Stephant, G. Louarn, M. Morsli, M. Hssein, Y. Mouchaal, S. Thouiri, M. Addou, A. Khelil, J. C. Bernède, *J. Phys. D. Appl. Phys.* **2017**, *50*, 375502.

[98] S. Khelifi, A. Belghachi, J. Lauwaert, K. Decock, J. Wienke, R. Caballero, C. . Kaufmann, M. Burgelman, *Energy Procedia* **2010**, *2*, 109.

[99] C. H. M. van der Werf, T. Budel, M. S. Dorenkamper, D. Zhang, W. Soppe, H. de Neve, R. E. I. Schropp, *Phys. Status Solidi - Rapid Res. Lett.* **2015**, *9*, 622.

[100] C. P. Lee, K. Y. Lai, C. A. Lin, C. T. Li, K. C. Ho, C. I. Wu, S. P. Lau, J. H. He, *Nano Energy* **2017**, *36*, 260.

[101] V. R. Voggu, J. Sham, S. Pfeffer, J. Pate, L. Fillip, T. B. Harvey, R. M. Brown, B. A. Korgel, *ACS Energy Lett.* **2017**, *2*, 574.

[102] B. Wang, L. L. Kerr, *Sol. Energy Mater. Sol. Cells* **2011**, *95*, 2531.

[103] F. Bella, D. Pugliese, L. Zolin, C. Gerbaldi, *Electrochim. Acta* **2017**, *237*, 87.

[104] M. Dasari, P. R. Rajasekaran, R. Iyer, P. Kohli, *J. Mater. Res.* **2016**, *31*, 2578.

[105] L. J. Pegg, R. A. Hatton, *ACS Nano* **2012**, *6*, 4722.

[106] H. Li, X. Liu, W. Wang, Y. Lu, J. Huang, J. Li, J. Xu, P. Fan, J. Fang, W. Song, *Sol. RRL* **2018**, 1800123.

[107] S. Castro-Hermosa, S. K. Yadav, L. Vesce, A. Guidobaldi, A. Reale, A. Di Carlo, T. M. Brown, *J. Phys. D. Appl. Phys.* **2017**, *50*, 033001.

[108] T. S. Kim, S. I. Na, S. S. Kim, B. K. Yu, J. S. Yeo, D. Y. Kim, *Phys. Status Solidi - Rapid Res. Lett.* **2012**, *6*, 13.

[109] L. La Notte, P. Cataldi, L. Ceseracciu, I. S. Bayer, A. Athanassiou, S. Marras, E.

Villari, F. Brunetti, A. Reale, *Mater. Today Energy* **2018**, *7*, 105.

[110] M. Smeets, K. Wilken, K. Bittkau, H. Aguas, L. Pereira, E. Fortunato, R. Martins, V. Smirnov, *Phys. Status Solidi Appl. Mater. Sci.* **2017**, *214*.

[111] K. Fan, T. Peng, J. Chen, X. Zhang, R. Li, *J. Mater. Chem.* **2012**, *22*, 16121.

[112] M. A. Osman, B. A. Keller, *Appl. Surf. Sci.* **1996**, *99*, 261.

[113] M. E. Schrader, *J. Colloid Interface Sci.* **1984**, *100*, 372.

[114] H. M. Stec, R. A. Hatton, *ACS Appl. Mater. Interfaces* **2012**, *4*, 6013.

[115] D. Alemu, H. Y. Wei, K. C. Ho, C. W. Chu, *Energy Environ. Sci.* **2012**, *5*, 9662.

[116] T. M. Brown, J. S. Kim, R. H. Friend, F. Cacialli, R. Daik, W. J. Feast, *Appl. Phys. Lett.* **1999**, *75*, 1679.

[117] B. Anothumakkool, I. Agrawal, S. N. Bhange, R. Soni, O. Game, S. B. Ogale, S. Kurungot, *ACS Appl. Mater. Interfaces* **2016**, *8*, 553.

[118] C. Gao, S. Yuan, K. Cui, Z. Qiu, S. Ge, B. Cao, J. Yu, *Sol. RRL* **2018**, *1800175*, 1800175.

[119] V. V. Tyagi, N. A. A. Rahim, N. A. Rahim, J. A. /L. Selvaraj, *Renew. Sustain. Energy Rev.* **2013**, *20*, 443.

[120] B. Burger, K. Kiefer, C. Kost, S. Nold, S. Philipps, R. Preu, J. Rentsch, T. Schlegl, G. Stryi-Hipp, G. Willeke, H. Wirth, W. Warmuth, *Photovoltaics Report*; Freiburg, 2018.

[121] M. A. Green, *J. Mater. Sci. Mater. Electron.* **2007**, *18*, 15.

[122] C. J. Brabec, *Sol. Energy Mater. Sol. Cells* **2004**, *83*, 273.

[123] A. Hagfeldt, G. Boschloo, L. Sun, L. Kloo, H. Pettersson, *Chem. Rev.* **2010**, *110*, 6595.

[124] P. V Kamat, *J. Phys. Chem. Lett.* **2013**, *4*, 908.

[125] N. G. Park, Perovskite solar cells: An emerging photovoltaic technology. *Mater. Today* **2015**, *18*, 65–72.

[126] J. Dagar, S. Castro-Hermosa, G. Lucarelli, F. Cacialli, T. M. Brown, *Nano Energy* **2018**, *49*, 290.

[127] F. De Rossi, T. Pontecorvo, T. M. Brown, *Appl. Energy* **2015**, *156*, 413.

[128] National Renewable Enery Laboratory, Perovskite efficiency chart. *NREL* **2018**.

[129] K. Miettunen, J. Vapaavuori, A. Tiihonen, A. Poskela, P. Lahtinen, J. Halme, P. Lund, *Nano Energy* **2014**, *8*, 95.

[130] M. Borghei, K. Miettunen, L. G. Greca, A. Poskela, J. Lehtonen, S. Lepikko, B. L. Tardy, P. Lund, V. (Ravi) Subramanian, O. J. Rojas, *Cellulose* **2018**, *25*, 3363.

[131] A. Punzi, A. Operamolla, O. H. Omar, A. D. Scaccabarozzi, G. M. Farinola, N. Stingelin, A. Punzi, A. Operamolla, O. H. Omar, F. Brunetti, D. Alberto, G. M. Farinola, N. Stingelin, **2018**.

[132] L. La Notte, D. Mineo, G. Polino, G. Susanna, F. Brunetti, T. M. Brown, A. Di Carlo, A. Reale, *Energy Technol.* **2013**, *1*, 757.

[133] F. Hoeng, A. Denneulin, J. Bras, *Nanoscale* **2016**, *8*, 13131.

[134] A. Fakharuddin, R. Jose, T. M. Brown, F. Fabregat-Santiago, J. Bisquert, *Energy Environ. Sci.* **2014**, *7*, 3952.

[135] T. M. Brown, F. De Rossi, F. Di Giacomo, G. Mincuzzi, V. Zardetto, A. Reale, A. Di Carlo, *J. Mater. Chem. A* **2014**, *2*, 10788.

[136] F. Bella, S. Galliano, M. Falco, G. Viscardi, C. Barolo, M. Grätzel, C. Gerbaldi, *Green Chem.* **2017**, *19*, 1043.

[137] V. Zardetto, G. De Angelis, L. Vesce, V. Caratto, C. Mazzuca, J. Gasiorowski, A. Reale, A. Di Carlo, T. M. Brown, *Nanotechnology* **2013**, *24*, 255401.

[138] K. H. Haas, *Adv. Eng. Mater.* **2000**, *2*, 571.

[139] P. Simon, Y. Gogotsi, *Nat. Mater.* **2008**, *7*, 845.

[140] G. Wang, L. Zhang, J. Zhang, *Chem. Soc. Rev.* **2012**, *41*, 797.

[141] D. Ge, L. Yang, L. Fan, C. Zhang, X. Xiao, Y. Gogotsi, S. Yang, *Nano Energy* **2015**, *11*, 568.

[142] G. P. Pandey, A. C. Rastogi, C. R. Westgate, *J. Power Sources* **2014**, *245*, 857.

[143] V. Kuzmenko, O. Naboka, M. Haque, H. Staaf, G. Göransson, P. Gatenholm, P. Enoksson, *Energy* **2015**, *90*, 1490.

[144] W. Liu, C. Lu, H. Li, R. Y. Tay, L. Sun, X. Wang, W. L. Chow, X. Wang, B. K. Tay, Z. Chen, J. Yan, K. Feng, G. Lui, R. Tjandra, L. Rasenthiram, G. Chiu, A. Yu, *J. Mater. Chem. A* **2016**, *4*, 3754.

[145] X. Yang, K. Shi, I. Zhitomirsky, E. D. Cranston, *Adv. Mater.* **2015**, *27*, 6104.

[146] S. Peng, L. Fan, W. Rao, Z. Bai, W. Xu, J. Xu, *J. Mater. Sci.* **2017**, *52*, 1930.

[147] M. Hilder, B. Winther-Jensen, N. B. Clark, *J. Power Sources* **2009**, *194*, 1135.

[148] G. Nystrom, A. Razaq, M. Stromme, L. Nyholm, A. Mihranyan, *Nano Lett.* **2009**, *9*, 3635.

[149] I. Ferreira, B. Brás, J. I. Martins, N. Correia, P. Barquinha, E. Fortunato, R. Martins, *Electrochim. Acta* **2011**, *56*, 1099.

[150] I. Ferreira, B. Brás, N. Correia, P. Barquinha, E. Fortunato, R. Martins, *IEEE/OSA J. Disp. Technol.* **2010**, *6*, 332.

[151] R. Martins, I. Ferreira, E. Fortunato, *Phys. Status Solidi - Rapid Res. Lett.* **2011**, *5*, 332.

[152] X. Zhang, J. Li, C. Chen, B. Lou, L. Zhang, E. Wang, *Chem. Commun.* **2013**, *49*, 3866.

[153] S. Berchmans, A. J. Bandodkar, W. Jia, J. Ramírez, Y. S. Meng, J. Wang, *J. Mater. Chem. A* **2014**, *2*, 15788.

[154] L. Hu, H. Wu, F. La Mantia, Y. Yang, Y. Cui, **2010**, *4*, 5843.

[155] L. Hu, N. Liu, M. Eskilsson, G. Zheng, J. McDonough, L. Wågberg, Y. Cui, *Nano Energy* **2013**, *2*, 138.

[156] Q. C. Liu, L. Li, J. J. Xu, Z. W. Chang, D. Xu, Y. Bin Yin, X. Y. Yang, T. Liu, Y. S. Jiang, J. M. Yan, X. B. Zhang, *Adv. Mater.* **2015**, *27*, 8095.

[157] A. G. Pandolfo, A. F. Hollenkamp, *J. Power Sources* **2006**, *157*, 11.

[158] G. A. Snook, P. Kao, A. S. Best, *J. Power Sources* **2011**, *196*, 1.

[159] M. Nilsson, M. Strømme, *J. Phys. Chem. B* **2005**, *109*, 5450.

[160] B. Winther-Jensen, N. B. Clark, *React. Funct. Polym.* **2008**, *68*, 742.

[161] T. Uesaka, *J. Pulp Pap. Sci.* **1991**, *17*, J39.

[162] M. R. E, *Handbook of physical and mechanical testing of paper and paperboard, volume 2*; Dekker Pubs, 1984.

[163] K. C.P., In *Advances in Biochemical Engineering/Biotechnology*; Springer, Berlin, Heidelberg, 1992; Vol. 45.

[164] L. Micheli, C. Mazzuca, A. Palleschi, G. Palleschi, *Anal. Bioanal. Chem.* **2012**, *403*, 1485.

[165] M. C. Area, H. Cheradame, *BioResources* **2011**, *6*, 5307.

[166] E. L. Williams, D. Grosjean, *J. Am. Inst. Conserv.* **1992**, *31*, 199.

[167] M. Hermenau, S. Schubert, H. Klumbies, J. Fahlteich, L. Müller-Meskamp, K. Leo, M. Riede, *Sol. Energy Mater. Sol. Cells* **2012**, *97*, 102.

[168] *Arjowiggings Tech. Pap.* **2014**, *Manufactur*.

[169] M. Roman, *Ind. Biotechnol.* **2015**, *11*, 25.

[170] L. Colombo, L. Zoia, M. B. Violatto, S. Previdi, L. Talamini, L. Sitia, F. Nicotra, M. Orlandi, M. Salmona, C. Recordati, P. Bigini, B. La Ferla, **2015**.

[171] Thintri Inc, Paper Electronics & Paper Batteries (2015) Source: https://www.researchandmarkets.com/research/6wwxlz/paper_electronics **2015**, 42.

[172] Editorial: A lesson on paper. *Nat. Electron.* **2018**, *1*, 429–429.

[173] Peter Harrop, Paper electronics is successful: where next? Source: https://www.idtechex.com/research/articles/paper-electronics-is-successful-where-next-00004185.asp) **2012**.

[174] J. Liu, C. Yang, H. Wu, Z. Lin, Z. Zhang, R. Wang, B. Li, F. Kang, L. Shi, C. P. Wong, *Energy Environ. Sci.* **2014**, *7*, 3674.

[175] A. J. Steckl, *IEEE Spectr.* **2013**, *50*, 48.

Author biographies

Francesca Brunetti

Francesca Brunetti received her PhD in Telecommunications and Microelectronics from the University of Rome Tor Vergata in 2005. In 2005, she was awarded of a Marie Curie Individual Fellowship spent in the Institute for Nanoelectronics of the Technical University of Munich, Germany.
Cofounder of the Centre for Hybrid and Organic Solar Energy and Associate Professor at the University of Rome Tor Vergata her current research is focused on the analysis, design and manufacture of electronic and optoelectronic devices through the use of nanomaterials (carbon nanotubes and graphene), organic semiconductors and perovskites realized on rigid and flexible substrates, including paper.

Alessandra Operamolla

Dr. Operamolla received her Ph.D. in Chemistry of Innovative Materials in 2009 from the University of Bari. She was a post-doctoral fellow between 2009 and 2015 at the Chemistry Department. She visited the Linz Institute for Organic Solar Cells, Austria, in 2008 and 2010, with an exchange grant received from the European Science Foundation. In 2016 she won the competitive FutureInResearch and was appointed Assistant Professor in Organic Chemistry at the Chemistry Department of the University of Bari, where she is presently carrying out independent research on nanocelluloses. Her research interests include novel organic semiconductors, self-assembled materials and organic-biologic hybrids.

Thomas M. Brown

Thomas M. Brown investigated OLEDs for his PhD at the Cavendish Laboratory, University of Cambridge. From 2001-2005 he developed OTFTs and E-paper as Senior Engineer at Plastic Logic Ltd. He was then recipient of a "Re-entry" Fellowship awarded by the Italian Ministry of University and Research. He is Associate Editor of Solar Energy. Cofounder of the Centre for Hybrid and Organic Solar Energy, and Associate Professor at the University of Rome-Tor Vergata, his current research is in in bio-hybrid devices and in perovskite solar cells, focusing especially on indoor light harvesting and on flexible substrates, including paper substrates.

The table of contents

Here we review progress regarding development of solar cells and energy storage devices on paper substrates where one or more of the main material layers are deposited via solution processing or printing. Paper is not only environmentally friendly and recyclable, it is thin, flexible, low-weight, biocompatible, and low-cost, also appealing as a substrate in the field of flexible printed electronics.

Keyword: flexible electronic, printed electronics paper, photovoltaics, energy storage, green electronics

Francesca Brunetti, Alessandra Operamolla, Sergio Castro-Hermosa, Giulia Lucarelli, Valerio Manca, Gianluca Farinola, and Thomas M. Brown*

Title: Printed solar cells and energy storage devices on paper substrates

ToC figure